PHYSICAL REVIEW
LETTERS

VOLUME 6 JANUARY 15, 1961 NUMBER 2

INTERPLANETARY MAGNETIC FIELD AND THE AURORAL ZONES*

J. W. Dungey†
Ionosphere Research Laboratory, The Pennsylvania State University, University Park, Pennsylvania
(Received November 10, 1960; revised manuscript received December 22, 1960)

The discovery[1] of a regular interplanetary magnetic field by Pioneer V has reawakened interest in Hoyle's[2] suggestion that the primary auroral particles are accelerated at neutral points in the combination of an interplanetary field and the geomagnetic field. Hoyle pointed out that the latitude of the aurora would depend on the distance of the neutral points from the earth and hence on the interplanetary field strength in the observed sense. The estimated particle energy was also reasonable. Dungey[3] discusses the accelerating mechanism. Here a qualitative model of the whole field is outlined and is found to be confirmed by the observed S_D current system.

Consider a model with interplanetary plasma moving relative to the earth, this "wind" lying approximately in the ecliptic plane, and an interplanetary field pointing roughly southward. The problem with no interplanetary magnetic field has been studied by several authors,[4] but the inclusion of this field alters the problem radically. The basic and awkward problem is that of the flow of plasma round the earth. This has not been solved but will be sketched using the physical picture of hydromagnetics. The flow in a plane containing the neutral points is shown in Fig. 1. The flow near the neutral points is controlled by the strong current density existing there (3). The reverse flow between the neutral points is important; it has to flow round the earth, but does so in a normal aerodynamic way. A steady laminar flow will be assumed here for simplicity, but it should be noted that large variations of the field were detected by Pioneer I.[5]

Denoting the local wind velocity by $\vec{u}$, the electric field $\vec{E}$ is approximately $-\vec{u}\times\vec{H}/c$ everywhere outside the ionosphere except near the neutral points. In a steady state $\vec{E}$ has a potential, which is constant on a line of force, with the same exceptions. Far from the earth $\vec{E}$ points out of the paper and the direction is still much the same near the neutral points and in the equatorial part of the region of reverse flow. In order to deduce the ionospheric currents, the topology of the magnetic field must be considered.

In Fig. 1 there will be two lines (not in the plane shown) connecting the neutral points and together forming an approximately circular closed curve C near the equatorial plane. The lines from one neutral point will cover a surface, topologically similar to half a cylinder, extend-

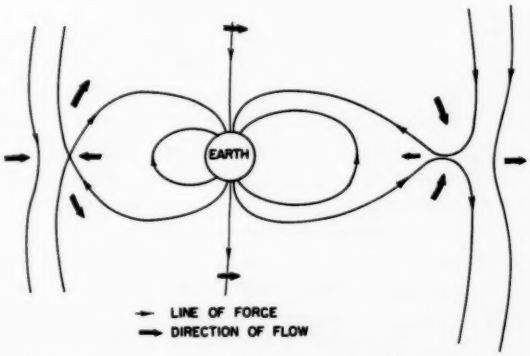

FIG. 1. Interplanetary plasma flow in a plane containing neutral points.

Copyright 1961 by the
American Physical Society

ing from C to infinity to the south and a surface like half a doughnut bounded by C and intersecting the earth's surface in a closed curve A in the northern hemisphere. The lines from the other neutral point complete the cylinder and doughnut and each neutral point has two lines on the other's surfaces. The cylinder and doughnut separate regions where lines of force have both, one, or no feet on the ground, the other ends going to infinity.

The plane of Fig. 1 is at constant potential by symmetry. Consider lines of force leaving the earth in a circle of longitude perpendicular to Fig. 1. The electric field fed in near the pole points out of the paper. Lines outside the curve A (that is, at lower latitude), however, pass through the equatorial plane and $\vec{E}$ here is out of the paper; following the potential up lines of force then gives a reversal of $\vec{E}$ at the curve A, because the lines from the equatorial plane have turned through more than 90°. Consequently the equipotentials in the ionosphere are as shown in Fig. 2. These equipotentials resemble the S_D current lines and the explanation is that Hall conductivity dominates in the ionosphere. Study of the conductivities σ_0, σ_1, and σ_2 in the ionosphere shows that the electric field will extend with only slight diminution down to the E layer, so that the integrated conductivity is appropriate and the current density is nearly perpendicular to $\vec{E}$. The phase of the current may be obtained by taking the direction of $\vec{j}\times\vec{H}$ at the pole to be opposite to that of $\vec{u}\times\vec{H}$ far out and then a wind

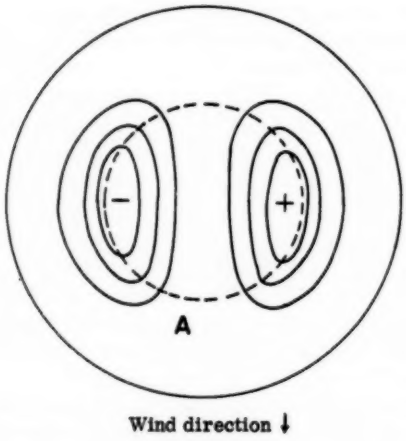

FIG. 2. Equipotentials in northern hemisphere for plasma winds of Fig. 1.

from the sun fits the observations.

The fit with observed S_D suggests the truth of the model. S_D must involve currents in the ionosphere driven from outside and the sudden reversal at the auroral zone seems to require neutral points. If the interplanetary field is northward the topology is quite different, the surface of lines of force enclosing the earth but not meeting it. It is therefore concluded that there is an approximately southward field.

One consequence of the flow in Fig. 1 is a mixing of the interplanetary plasma into the outer atmosphere, which will upset the equilibrium under gravity which would exist in the absence of such a flow. The whistler data suggest that plasma is being lost far out.[6]

The connection between the neutral points and auroras is obvious in this model, but it remains to study the motion of individual particles and the effect of turbulence. The outer Van Allen belt also remains to be discussed; the return flow in Fig. 1 must not upset its symmetry about the geomagnetic axis. The model predicts an asymmetry for auroras: for a wind from the sun there should be proton auroras before midnight and electron auroras after midnight. Recent results[7] from IGY data are of great interest in connection with the model presented here and promise substantial advances in our understanding of the subject.

---

*The research reported in this work has been sponsored by the Geophysics Research Directorate of the Air Force Cambridge Research Center, Air Research and Development Command, and, in part, by the National Science Foundation.

†Present address: Atomic Weapons Research Establishment, Aldermaston, England.

[1]P. J. Coleman, Jr., L. Davis, and C. P. Sonnett, Phys. Rev. Letters 5, 43 (1960).

[2]F. Hoyle, Recent Researches in Solar Physics (Cambridge University Press, New York, 1958), Sec. 27.

[3]J. W. Dungey, Cosmic Electrodynamics (Cambridge University Press, New York, 1958), Secs. 6.4 and 8.4.

[4]D. B. Beard, J. Geophys. Research 65, 3559 (1960).

[5]C. P. Sonett, Phys. Rev. Letters 5, 47 (1960); C. P. Sonett, E. J. Smith, and A. R. Smith, Proceedings of the First International Space Sciences Symposium, edited by H. K. Kallman Bijl (North Holland Publishing Company, Amsterdam, 1960), p. 921.

[6]R. L. Smith and R. A. Helliwell, J. Geophys. Research 65, 2583 (1960).

[7]T. N. Davis, J. Geophys. Research 65, 3497 (1960).

COSMIC-RAY NEUTRON INCREASE FROM A FLARE ON THE FAR SIDE OF THE SUN

H. Carmichael and J. F. Steljes
Atomic Energy of Canada Limited, Chalk River, Canada

D. C. Rose
Division of Pure Physics, National Research Council, Ottawa, Canada

and

B. G. Wilson
Sulphur Mountain Laboratory, University of Alberta, Calgary, Canada
(Received December 27, 1960)

Two conspicuous bursts of cosmic-ray neutrons produced by large visible solar flares were observed at many laboratories throughout the world on November 12 and 15, 1960, and these events are now being intensively studied. The purpose of this note is to draw attention to a third and rather inconspicuous injection of solar cosmic radiation that occurred on November 20, 1960, and to point out the interesting fact that the radiation in this case seems to have originated in a large unseen flare which occurred at a solar longitude some 120°W of the center of the solar disk; in fact, about 30° behind the west limb of the sun. The November 20 injection was noted in Canada at Deep River and at Sulphur Mountain and has been found to be present also in the Ottawa and Churchill neutron monitor data. Results from Resolute are not yet available.

The increase started at 2055±10 U.T. on November 20. The preliminary report of solar activity[1] does not list any large flare such as in the past has always been seen at the time of a sea level solar cosmic-ray increase, while the listing of numerous small flares shows that observing conditions were good. The most likely place for a large flare to have occurred was McMath plage region 5925 which had already produced major flares (of importance 3 and 3+) on November 10, 12, and 15. This region was still active as it passed round the west limb with loops, surges, and a succession of small flares. Assuming a 27-day rotation period and taking the 3+ flare at 1322 U.T. November 12 at 10°W of the center of the solar disk,[2] the corresponding position for 2055 U.T. on November 20 is 120°W and we postulate that a major solar flare occurred there about that time.

This postulate is strongly supported by the observations of solar radio noise made by Covington[3] and analyzed in the accompanying Letter.[4]

Detection of solar radio noise requires line-of-sight propagation from the source to the observing station and consequently noise outbursts are observed with comparable frequency from both the east and the west half of the solar disk. In the case of solar cosmic rays, however, it has been noted that solar cosmic radiation seldom reaches the earth from flares near the center and on the eastern half of the disk. If it does, the signal shows characteristically a very slow rise. From flares on the west half the increases, whenever they occur (only 10 solar increases in all at sea level prior to the one being discussed have been recognized in the past 20 years), are fast rising and tend to start sooner in relation to the time of the visible flare. This behavior has recently been[5] attributed to the existence of configurations of magnetic lines of force above a strongly active solar region which stretch in an easterly curving path, as a result of the rotation of the sun, from the sun to beyond the orbit of the earth. In the present case we must assume that these magnetic lines of force formed an easy path to the earth for high-energy protons generated some way behind the western limb of the sun.

The evidence for a neutron increase due to solar cosmic rays is exhibited in Fig. 1. The pressure-corrected hourly totals measured by the standard neutron monitor at Deep River cover a period of 15 days immediately following the solar cosmic-ray increase of November 15. During this period the intensity is recovering from the Forbush decreases that occurred on November 12, 13, and 15. Large diurnal and other slow fluctuations are apparent. There is also a small Forbush decrease at 0000 U.T. on November 25. At 2100 hours Universal Time on November 20 (Fig. 1) a sudden increase of neutrons is to be seen at Sulphur Mountain, Deep River (Ottawa is similar), and at Churchill, but the mesons at Sulphur Mountain did not exhibit a corresponding[6] increase. It is also evident from Fig. 1 that the sudden neutron increase at Sulphur Mountain (altitude 2283 m), relative to the normal count

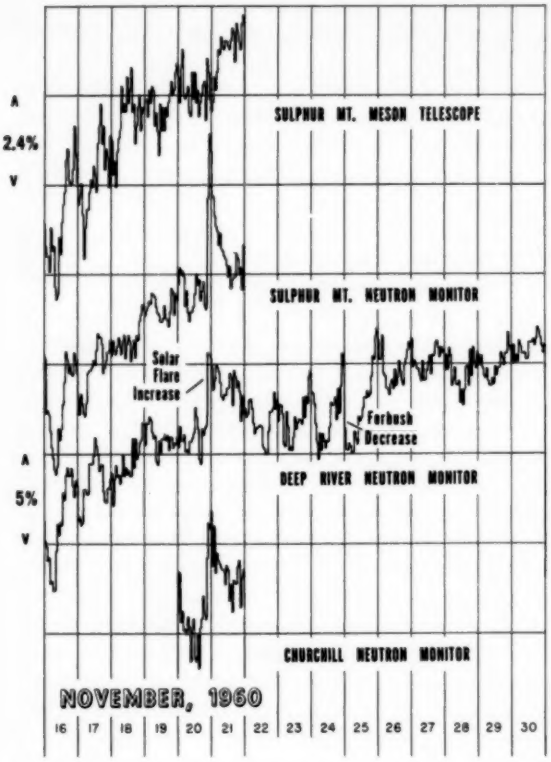

FIG. 1. Pressure-corrected hourly totals from standard neutron monitors and from a meson telescope. The ordinate scale divisions are at intervals of approximately 5% for the neutron monitor graphs and 2.4% for the meson telescope graph.

rate there, was more than double the size of the increase seen at the sea level stations. The characteristic shape of this increase, the fact that it was relatively much larger at a mountain station, and its absence in a meson telescope at that same station, indicate that it was produced by solar protons.

The Sulphur Mountain and Deep River neutron totals are plotted on an expanded time scale in Fig. 2 to show the shape of the increase. For this figure the neutron counting rate at Deep River

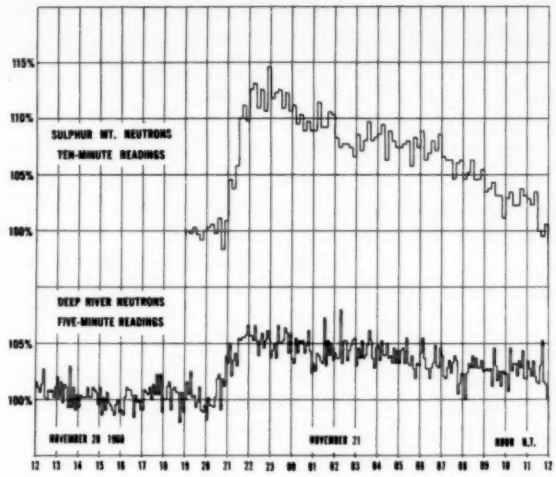

FIG. 2. Uncorrected 10-minute totals for Sulphur Mountain and pressure-corrected 5-minute totals for Deep River. The basic (i.e., 100%) rates for these graphs are 100 600 per hour at Sulphur Mountain and 149 000 per hour at Deep River.

has been more than doubled by including the counts from a graphite-moderated neutron monitor. From Fig. 2 the onset of the increase appears to have been at 2055 ± 10 U.T. and the rise to maximum took about one hour.

---

[1]Billings, Trotter, and Wetmore, High Altitude Observatory Preliminary Report on Solar Activity, Boulder, Colorado, 1960 (unpublished).

[2]Helen Dodson-Prince, McMath-Hulbert Observatory (private communication, November, 1960).

[3]Daily values of solar flux at 2800 Mc/sec (10.7 cm) and outstanding events recorded at National Research Council, Ottawa, Canada, in November 1960; December, 1960.

[4]A. E. Covington and G. A. Harvey, following Letter [Phys. Rev. Letters 6, 51 (1960)].

[5]K. G. McCracken and R. A. R. Palmeira, J. Geophys. Research 65, 2673 (1960); and references therein.

[6]Note that the vertical percentage scale on which the meson totals are plotted in Fig. 1 has been expanded with respect to that used for the neutron graphs by a factor 2.1 to make the general variations look the same.

10.7-cm SOLAR NOISE BURST OF NOVEMBER 20, 1960

Arthur E. Covington and Gladys A. Harvey
Radio and Electrical Engineering Division, National Research Council, Ottawa, Canada
(Received December 27, 1960)

The occurrence of a flare upon the far side of the sun as described in the previous Letter by Carmichael et al.[1] is an extremely likely event as inferred from analysis of two sets of 10.7-cm solar noise observations taken at the Radio Observatory of the National Research Council, Ottawa, Canada.

The first set of observations was made with a 1.3-meter parabolic reflector and a radiometer which records the solar emission from the whole disk from sunrise to sunset. A tracing of the pertinent portion of the record for November 20, 1960 from 19:00 U.T. to 22:00 U.T., is shown in Fig. 1. The burst is the enhancement above the daily quiet level—shown by the dotted line and estimated from the level on the previous day. The burst features from 20:30 until sunset at 21:20 have been modified by the interference pattern formed by the direct solar ray and the ray reflected from the earth. The times of start of the main burst features are given in Table I. The preliminary listing of flares[2] for this period has been examined and the times of start of the six flares reported in this period are also listed in Table I. The flares occurred in two regions—

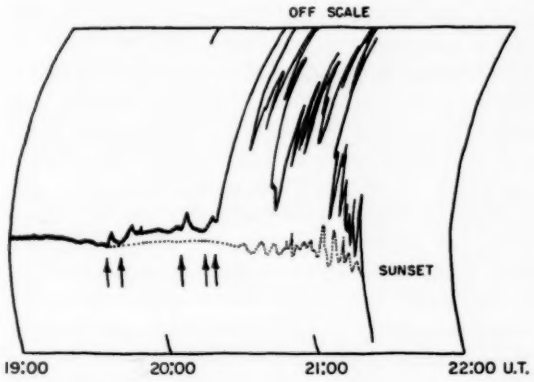

FIG. 1. Record of 10.7-cm solar noise burst, November 20, 1960.

one, the very active region of interest (*HH* 25); the other, a smaller region in the same latitude as *HH* 25 but following it by a few days (*FF* 32).

Comparison of the times of start of the bursts and flares within the time interval customarily used for associating 10-cm bursts and flares show that two of the flares, 20:09 and 20:19,

Table I. Comparison of flare and burst features.

Flare features			Burst features		
Beginning	Importance	Region	Beginning	Flux	Remarks
19:27	1-	*FF* 32			No evidence of flux increase.
			19:39	7	Small rise and fall of flux.
			19:45	7	Small rise in flux to a steady level.
19:55	1-	*FF* 32			No evidence of flux increase.
20:09	1-	*FF* 32	20:09	11	Small rise and fall of flux on steady level.
20:16	1-	*FF* 32			No evidence of flux increase.
20:17	1-	*HH* 25			No evidence of flux increase.
20:19	1	*HH* 25	20:19	7	Small rise in flux; no appreciable fall.
			20:23	400[a]	Large increase in flux; continuing until end of observations.

[a] Peak value obtained from low gain–high speed channel. Not illustrated.

coincide well with burst features. The lesser of these, at 20:09, occurs in the lesser and following region (*FF* 32) which is just inside the limb around which the main region (*HH* 25) is disappearing. The larger flare, at 20:19, occurs in the main region (*HH* 25) which at this time is mostly around the limb. The other small flares are not associated in time with any burst features—which is not unusual, in that this is the case for the majority of the smallest flares. The unusual feature of the burst at 20:23 is that this is a radio event of more than average intensity with a flux of 400×10^{-22} (watt/m^2)/cps and a duration of over 45 minutes, while the only flare listing for approximately this time is of importance 1 and duration 4 minutes. Comparison of 10-cm events and flares over a long period of time has indicated that bursts of this magnitude are almost always associated with flares of importance 2 at least. This supports the suggestion of an intense flare on the far side of the sun occurring in the active region which has largely disappeared around the limb. Possibly the short-duration flare reported is a small fragment on the limb of the much larger hidden flare.

A similar situation was observed previously on June 9, 1959. Analysis[3] showed in this case that the hidden flare occurred in a region which was just about to appear on the eastern limb. In this critical position, a direct line of sight is possible only for the radio emissions which are produced in elevated regions above the flare. It has also been suggested[4] that this event produced x-ray emissions.

The second set of solar noise observations was made with a 185-meter aperture interferometer system with a fan-shaped beam 1′ E.W. by 2° N.S. The daily strip scans of the solar surface are made at 16:30 U.T. and enable the bright radio emissive regions to be accurately located in one dimension. On November 4, a radio emissive region appeared on the eastern limb, crossed the central meridian on November 12, and was last seen on the western limb on November 20. The relation of the trajectory of the radio emissive region with respect to the solar disk indicates that the region was 20° to 30° north of the solar equator. This corresponds to the location of the optical region *HH* 25. In addition, the scan taken during the post-burst increase associated with the November 12 eruption clearly indicates increased emission from this region. Examination of the provisional sunspot positions as reported by the U. S. Naval Observatory showed that the sunspots of this region were first seen near the eastern limb on November 6 and last seen on the western limb on November 18. The longer visibility of the radio region in comparison with the optical manifestations is typical[5] and shows again that the 10-cm radio emission is observed even when the optical center is located on the far side of the limb. This emission is from a hot coronal condensation located some 3% of the solar radius above the photosphere. The surface area of the radio region seems related to bright plages with observed E. W. extents ranging from 1 to 6 minutes of arc.

When the reported sunspot positions are projected to give a value for November 20, it is found that the region extends from 20° to 30° around the far side of the western limb. Since radio emission from the coronal condensation in this position was observed, it is reasonable to assume, in the absence of an intense flare on the visible disk, that a hidden intense flare was responsible for the burst of noise observed at 20:23 U.T.

---

[1]H. Carmichael, J. F. Steljes, D. C. Rose, and B. G. Wilson, preceding Letter [Phys. Rev. Letters 6, 49 (1961)].

[2]Billings, Trotter, and Wetmore, High Altitude Observatory Preliminary Report on Solar Activity, Boulder, Colorado, 1960 (unpublished).

[3]R. J. Coates, A. E. Covington, and S. Edelson, Astron. J. 64, 326 (1959).

[4]J. Kleczek and L. Krivsky, Nature 186, 1035 (1960).

[5]A. E. Covington and G. A. Harvey, Astrophys. J. 132, 435 (1960).

HIGH-FREQUENCY POTENTIAL WELL FOR DENSE PLASMAS*

Albert J. Hatch
Argonne National Laboratory, Argonne, Illinois
(Received December 27, 1960)

The stable dynamic containment of charged particles and low-density plasmas in nonhomogeneous high-frequency electric or electromagnetic fields is now firmly established theoretically[1-3] and experimentally.[4-6] In electromagnetic fields the containing force on electrons is derivable from a potential function[3]

$$\Phi = (e^2/4m\omega^2)\langle E^2\rangle_{av}. \quad (1)$$

Here e and m are the charge and mass of the electron, ω is the radian frequency of the field, and $\frac{1}{2}\langle E^2\rangle_{av}$ is the time-averaged square of the electric field $\langle \vec{E}\cdot\vec{E}\rangle_{av}$, where $\vec{E} = E\exp(j\omega t)$. This scalar point function generates three-dimensional potential wells in the vicinity of the central field nodes in certain resonant-cavity standing wave modes such as the electric quadrupole mode. Because of the necessity that the field penetrate the plasma in order to act on the individual particles, the plasma density is limited to values which make $\omega_p > \omega$, where $\omega_p = (ne^2/m\epsilon_0)^{1/2}$ is the characteristic radian frequency of the plasma and n is the electron density. Consequently, there has been only mild interest in the basic and applied aspects of Φ potential wells.

The purpose of this Letter is to describe a newly recognized absolute potential well which theoretically appears to be capable of containing dense plasmas ($\omega_p > \omega$), and thus does not suffer from the density limitation imposed on the Φ well. The present analysis arose out of theoretical considerations of the results of an experimental analog study of the equilibrium properties of simulated plasma cores in resonant cavity fields.[7]

If a small volume of sharply bounded dense neutral plasma is placed in a resonant cavity field, the penetration of the high-frequency E and H fields into the highly conducting volume of plasma will be limited to a very small skin depth. It is therefore convenient to consider the interior volume of the plasma as field free and to assume that the plasma can be represented by a small rigid neutral conducting sphere. This sphere can be considered as a test volume whose successful containment by a particular cavity mode indicates the strong possibility of similar containment by that same mode of a somewhat larger, less well defined, nonrigid, nonspherical volume of dense plasma.

The potential of a perfectly conducting sphere in a quasi-static parallel E field[8] is $U_e = -\pi r_0^3 \epsilon_0 \langle E^2\rangle_{av}$. Similarly, for a perfectly diamagnetic sphere in a quasi-static parallel H field the potential is $U_m = \frac{1}{2}\pi r_0^3 \mu_0 \langle H^2\rangle_{av}$. The net potential of this sphere in superposed parallel E and H fields is therefore

$$\Upsilon = \pi r_0^3 (\tfrac{1}{2}\mu_0 \langle H^2\rangle_{av} - \epsilon_0 \langle E^2\rangle_{av}). \quad (2)$$

This expression appears in the theory for the measurement of cavity fields by frequency perturbation due to the presence of a small metallic sphere[9] and therefore is not new in itself. The new step reported here involves the use of Υ as a field property with which the containment capabilities of various resonant-cavity field configurations can be assessed. In order to apply Eq. (2) to the nonuniform fields in cavities it is necessary that $r_0/\lambda \ll 1$, where $\lambda = 2\pi c/\omega$, to insure that the local fields in which the sphere is placed be approximately parallel. The net average body force acting on the sphere is $-\Delta\Upsilon$ which phenomenologically is due to the dielectrophoretic and diamagnetic behavior of the sphere in the nonhomogeneous field. Various aspects of the significance of this force to the containment problem have been discussed recently by Yankov.[10]

The exact calculation of Υ is greatly simplified by letting r_0 approach 0, in which case Υ becomes a scalar point function of a point sphere. Υ has been calculated for several spherical cavity modes for which the field components $E(r, \theta, \phi)$ and $H(r, \theta, \phi)$ are given in standard references,[11] namely, electric dipole (TM_{110}), magnetic dipole (TE_{110}), electric quadrupole (TM_{210}), magnetic quadrupole (TE_{210}), and magnetic sextupole (TE_{310}). Of these modes only the last two possess suitable absolute potential wells, and only the TE_{210} mode well is here discussed in detail. (A comprehensive report on the various modes is in preparation.)

The field structure of the TE_{210} magnetic quadrupole mode in the spherical cavity is shown qualitatively in Fig. 1. This is a cross section of the field in the (r, θ) plane. The broken lines represent the H field, and the dots and crosses

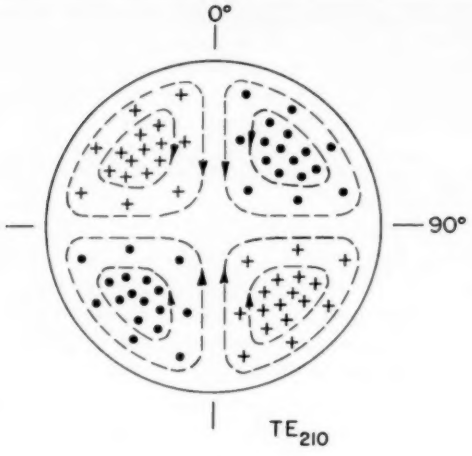

FIG. 1. Field configuration of the TE_{210} magnetic quadrupole mode in a spherical cavity. Magnetic field lines are shown as broken lines; the dots and crosses represent the electric field.

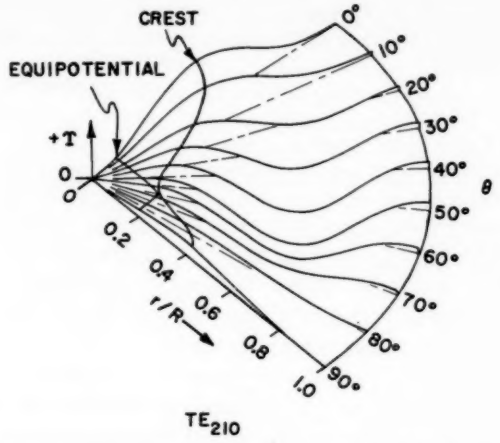

FIG. 2. Potential function $\Upsilon(r,\theta)$ in the TE_{210} magnetic quadrupole mode in a spherical cavity. The potential well lies between the origin and the crest, and is symmetrical in the four quadrants.

represent the E field whose lines are concentric circles centered on the polar axis. There is a node in both the E and H fields at the center of the cavity.

Values of $\Upsilon(r,\theta)$ for the magnetic quadrupole mode in a sphere of radius R are shown in Fig. 2 for the upper right quadrant only. The radial variation of Υ has been plotted on an arbitrary scale at 10° increments of θ. In each curve Υ is zero at the center of the cavity where there is a field node, becomes positive for small values of r/R, and reaches a crest in the vicinity of $0.20 < r/R < 0.43$ as shown in Fig. 2. The minimum crest height occurs at $r/R = 0.215$, $\theta = 65°$; the maximum crest height is on the polar axis, $\theta = 0°$, at $r/R = 0.43$. The crest at the equator, $\theta = 90°$, also occurs at $r/R = 0.43$. The ratio of the maximum to the minimum crest height is approximately 9:1. The well thus formed inside the Υ crest is symmetrical in the four quadrants. The volume of the well inside the crest is 2.6% of the volume of the cavity; the volume of that portion of the well enclosed within the equipotential drawn through the minimum crest point, as shown in Fig. 2, is 0.6% of the volume of the cavity. Neither of the configurations suggested by the crest or by the equipotential contours are necessarily indicative of the configuration of a finite dense plasma contained in the well. Indeed, the work of Berkowitz et al.[12] indicates that a more likely configuration is that of a hypocycloid of revolution. The apparent well in the vicinity of $r/R = 0.6$ and $\theta = 50°$ occurs at an E-field maximum rather than at a field node, hence is unsuitable for containment of dense plasmas.

The necessary conditions for the existence of an absolute Υ well are that there be a point in the electromagnetic field where (a) $\Upsilon = E = H = 0$, (b) $\partial\Upsilon/\partial r = 0$, and (c) $\partial^2\Upsilon/\partial r^2 > 0$. Consideration of the field structure of the various modes in simple cavities (i.e., spherical, cylindrical, or rectangular) indicates that the above conditions exist simultaneously only in the magnetic quadrupole and higher order magnetic multipole modes. It is significant that the magnetic quadrupole mode is the resonant cavity version of the static magnetic "cusp" field which has been shown[12] to have stable equilibrium properties for the containment of dense plasmas. The present result is also consistent with the levitation experiments in audio-frequency magnetic quadrupole fields described by Okress et al.,[13] and provides an alternate explanation of the phenomena which they observed.

The existence of the Υ wells (and hills) indicates the possibility of new basic phenomena involving the interaction of plasmas with electromagnetic fields and suggests new approaches to the applied problem of the containment of dense plasmas. In either case one must go beyond the present analysis and consider additional factors such as the effects of coexisting Φ potential wells or hills, high rf power requirements (of the order of kilowatts to produce pressures of dynes/cm^2),

competition from other effects, and alteration of the Υ well by the finite size of a contained plasma core. In regard to this last point, consideration of the analog experiment[7] (unpublished results) and the levitation experiment[13] indicates that an Υ well exists for test-sphere diameters up to about $r_0/R \leq 0.1$ in the present case.

It is a pleasure to thank A. Strecok for programming the computations, and G. R. Ringo and F. E. Throw for helpful comments.

*Work performed under the auspices of the U. S. Atomic Energy Commission.

[1]M. L. Good, University of California Radiation Laboratory Report UCRL-4146, 1953 (unpublished).

[2]H. A. H. Boot, S. A. Self, and R. B. R. Shersby-Harvie, J. Electronics and Control 4, 434 (1958).

[3]A. V. Gapanov and M. A. Miller, J. Exptl. Theoret. Phys. (U.S.S.R.) 34, 242 (1958) [translation: Soviet Phys.-JETP 7, 168 (1958)].

[4]R. F. Wuerker, H. Shelton, and R. V. Langmuir, J. Appl. Phys. 30, 342 (1959).

[5]M. A. Miller, J. Exptl. Theoret. Phys. (U.S.S.R.) 35, 299 (1958) [translation: Soviet Phys.-JETP 8, 206 (1959)].

[6]S. A. Self and H. A. H. Boot, J. Electronics and Control 6, 527 (1959).

[7]A. J. Hatch and J. W. Butler, Bull. Am. Phys. Soc. 5, 324 (1960).

[8]J. A. Stratton, Electromagnetic Theory (McGraw-Hill Book Company, New York, 1941), p. 206.

[9]L. C. Maier and J. C. Slater, J. Appl. Phys. 23, 68 (1952).

[10]V. V. Yankov, J. Exptl. Theoret. Phys. (U.S.S.R.) 36, 560 (1959); 37, 224 (1959) [translation: Soviet Phys.-JETP 9, 388 (1959); 10, 158 (1960)]; J. Tech. Phys. (U.S.S.R.) 30, 1019 (1960).

[11]Reference 8, p. 555.

[12]J. Berkowitz, K. O. Friedrichs, H. Goertzel, H. Grad, J. Killeen, and E. Rubin, Proceedings of the Second United Nations International Conference on the Peaceful Uses of Atomic Energy (United Nations, Geneva, 1958), Vol. 31, p. 171.

[13]E. C. Okress, D. M. Wroughton, G. Comenetz, P. H. Brace, and J. C. R. Kelly, J. Appl. Phys. 23, 545 (1952).

ASPHERICAL 3*d* ELECTRON DISTRIBUTION IN Ni^{++}†

Harvey A. Alperin

U. S. Naval Ordnance Laboratory, Silver Spring, Maryland and
Brookhaven National Laboratory, Upton, New York

(Received December 22, 1960)

The purpose of this Letter is to report the results of the first measurement of an aspherical magnetic form factor of an antiferromagnetic single crystal, nickel oxide, using unpolarized neutrons. The simple structure, if this compound is purely ionic, makes it possible to explain the resultant e_g symmetry that is obtained. This differs from previous (polarized beam) measurements[1-4] where no simple explanation of the asymmetries is possible because the materials studied were either metals or (in one case) had the complicated spinel structure. The form factor of Ni^{++} is found to lie above the free-atom curve in contrast to the case of Mn^{++} where the converse is true. These results are of interest because of the very recent Hartree-Fock spin polarized calculations for Ni^{++} by Watson and Freeman.[5]

Unpolarized neutrons were used since the more accurate polarized neutron beam technique[6] is not applicable to antiferromagnets like NiO that do not have superimposed nuclear and magnetic reflections. The single crystal used for this investigation was cut in the shape of a cylinder (8 mm high, 2.3 mm in diameter) from a large boule grown by flame fusion. Integrated intensities of all nuclear and magnetic reflections were measured at room temperature up to a value of $\sin\theta/\lambda = 0.78$ using a wavelength of 1.046 A. From the heavily extinguished nuclear reflections a mosaic spread parameter of 112 seconds of arc was determined. This resulted in secondary extinction corrections to the magnetic intensities of only 12% for the strongest reflection (111), of only 3% for the next strongest ($\bar{3}11$), and of a completely negligible amount for all the other weaker reflections which occur at higher Bragg angles.

Effects due to double Bragg scattering became particularly noticeable when measuring the very weak outer reflections (signal to noise ratios in the range 0.05 to 0.1). In order to help correct for these effects, additional room temperature measurements were taken at a second wavelength of 1.005 A. By taking account of the changes that occurred in the peak shapes upon changing the

wavelength, it was possible to obtain estimates of the true intensity of the reflections under study. However, in many cases the error entailed in this procedure was rather large.

The experimental values for the magnetic form factor are plotted in Fig. 1 as the circles. The values were put on an absolute scale by using the previous result[7] that the value of the form factor for the (111) reflection is 0.94. The important observation to be made is that values of the form factor are obtained which depart radically from a smooth curve. In particular, outer reflections which occur at the same Bragg angles show very different values for their form factors. The existence of such a multivalued form factor demonstrates that the unpaired $3d$ electrons are distributed aspherically about each Ni^{++} ion.

To investigate the possibility (however unlikely) that the observed results might be due to the effect of anisotropic motions, either of the atoms with respect to one another or of the atoms with respect to their electron clouds, the $(\bar{1}1, 1, 1)$ and $(\bar{5}, 7, 7)$ reflections, which occur at the same Bragg angle, were measured after cooling the crystal to 117°K. If the effect were due to anisotropic vibrations one would expect the ratio of the form factors of the two reflections to approach approximately unity as the temperature approaches 0°K. Within the limits of experimental error, this ratio did not change upon cooling from 297°K to 117°K.

The aspherical unpaired $3d$ electron distribution observed experimentally is just what is expected due to the splitting of the energy levels of the d electrons in the field of the anions. According to crystal field theory,[8] in an electric field of octahedral symmetry the five-fold degenerate levels split into a low-lying triplet of t_{2g} symmetry and a higher doublet of e_g symmetry. Since the levels fill up according to Hund's rule, the two unpaired electrons which give rise to the magnetic moment should then exhibit pure e_g symmetry.[9]

The form factor can be written as the sum of a spherical part and an aspherical part, $f = f_S + f_A$. The part f_A (having pure e_g symmetry in our case) can be calculated following the methods of Weiss and Freeman.[10] However, in order to compare the experimental results directly with those predicted for an f_A of e_g symmetry, it is necessary first to determine f_S. Since at the present time there is no adequate way of calculating f_S for atoms bound in a solid, f_S was chosen to yield the best agreement between the experimental and calculated values of the form factor. It was found to be possible (also most convenient and instructive) to do this by scaling the free-atom spherical form factor[11] for Ni^{++}, i.e., $f_S(x) = f_0(kx)$, where f_0 is the free-atom form factor, $x = \sin\theta/\lambda$, and the scale factor $k = 0.83$. In Fig. 1, f_S is plotted as the solid curve.[12] The final calculated values of f are denoted by the

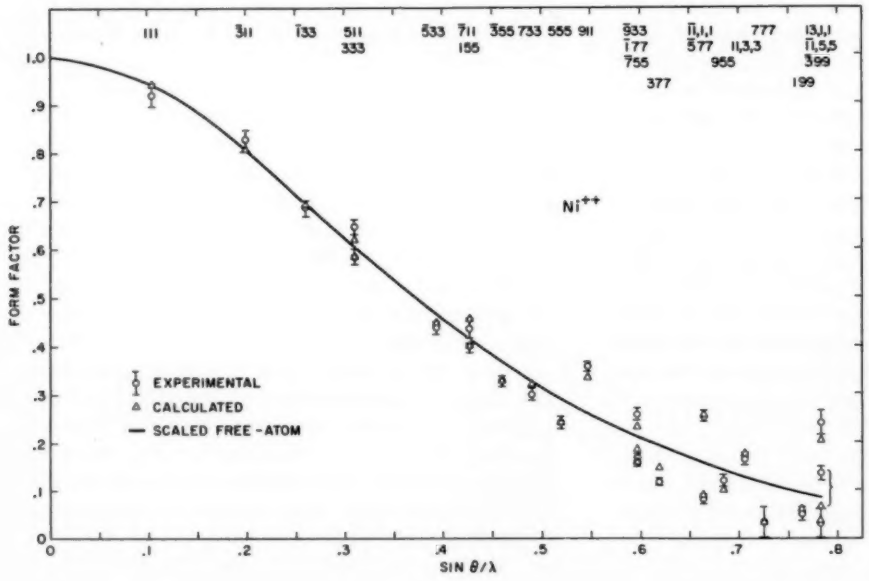

FIG. 1. The magnetic form factor of Ni^{++} in nickel oxide. The indices at the top of the figure refer (in the order shown) to the reflections directly below.

triangles. Reasonable agreement is thus obtained between the experimental form factor values and those computed assuming the unpaired electrons to be in a state of pure e_g symmetry.

It is important to observe that the scale factor, k, here determined experimentally, is such as to make the unpaired $3d$ charge distribution for Ni^{++} much more compact in the solid than it is for the free atom. This is in contrast to the case of Mn^{++} where experiments[13] show that the charge distribution is expanded in the solid.

These experimental results may be compared with the recent calculations of Watson and Freeman[5] for the Ni^{++} ion. These Hartree-Fock self-consistent field calculations allow the wave functions of electrons with opposite spins to have different radial dependencies (spin polarization) and lead to a contraction of the charge distribution (both for the free-atom case and the case where the Ni^{++} ion is placed in an octahedral array of point charges).[14] Unfortunately, the magnitude of the contraction is much too small to explain the observations reported here. Nevertheless, the important fact that the relation of the observed f_S to the free-atom f_S is just opposite for the cases of Ni^{++} and Mn^{++} would lead one to look for the origin of this effect in the outstanding difference between the two ions: namely their differing spin configurations. These experimental results also serve to suggest that whereas effects such as spin polarization and crystalline environment have a large influence on f_S, their effect on f_A is small.

The author wishes to thank Professor E. Uchida and Dr. Y. Nakazumi for the single crystal of NiO.

---

†Performed under the auspices of the U. S. Atomic Energy Commission.

[1]R. Nathans, C. G. Shull, G. Shirane, and A. Andresen, J. Phys. Chem. Solids 10, 138 (1959).

[2]R. Nathans and A. Paoletti, Phys. Rev. Letters 2, 254 (1959).

[3]S. J. Pickart and R. Nathans, Suppl. J. Appl. Phys. 31, 372S (1960).

[4]R. Nathans, S. J. Pickart, and H. A. Alperin, Bull. Am. Phys. Soc. 5, 455 (1960).

[5]R. E. Watson and A. J. Freeman, Phys. Rev. 120, 1125 (1960); R. E. Watson and A. J. Freeman, Phys. Rev. 120, 1134 (1960).

[6]R. Nathans, Suppl. J. Appl. Phys. 31, 350S (1960).

[7]H. A. Alperin, U. S. Naval Ordnance Laboratory Report NAVORD-6907, June, 1960 (unpublished).

[8]J. D. Dunitz and L. E. Orgel, J. Phys. Chem. Solids 3, 20 (1957).

[9]We are assuming here that the radial part of the wave functions is the same for all eight electrons so that the three electrons of t_{2g} symmetry with their spins in one direction "cancel" the three electrons of like symmetry with oppositely directed spins.

[10]R. J. Weiss and A. J. Freeman, J. Phys. Chem. Solids 10, 147 (1959).

[11]R. E. Watson and A. J. Freeman, Acta Cryst. (to be published).

[12]The form factor of Ni^{++} in $KNiF_3$ has been measured up to the value $\sin\theta/\lambda = 0.32$ by V. Scatturin, L. Corliss, N. Elliott, and J. Hastings, Acta Cryst. (to be published). Their result, which is for a powder measurement, is in approximate agreement with the curve presented here.

[13]J. M. Hastings, N. Elliott, and L. M. Corliss, Phys. Rev. 115, 13 (1959).

[14]It should be noted that Mn^{++} which has all its spins in the same direction has no spin polarization effect.

TUNNELLING FROM A MANY-PARTICLE POINT OF VIEW*

J. Bardeen
University of Illinois, Urbana, Illinois
(Received December 16, 1960)

Giaever[1] and more recently Nicol, Shapiro, and Smith[2] have observed the tunnelling current flowing between two metals separated by a thin oxide layer. The most interesting results are obtained when one or both of the metals are superconducting, in which case they find direct evidence for a gap in the quasi-particle spectrum of the superconductor. They were able to account for the data quantitatively on the assumption that the only relevant factor is the density of states in energy. This is to be expected if the transition probability for transfer of an electron from one side to the other is given by the familiar expression $(2\pi/\hbar)|M|^2\rho_f$, where M is the matrix element and ρ_f the energy density of final states, and if it is further assumed that M can be treated as a constant. It is implied that M is not only independent of energy for the small energy differences involved, but is also unchanged when the metal goes from normal to superconducting.

However, it is not immediately obvious that these assumptions are justified. We give here a discussion of tunnelling from a many-particle point of view and show that it is plausible to treat M as a constant in the interpretation of the experiments.

We suppose that the barrier extends from x_a to x_b, with metal a to the left of x_a and metal b to the right of x_b. Consider two many-particle states of the entire system, Ψ_0 and Ψ_{mn}, which differ in the transfer of an electron from a to b. We suppose that Ψ_0 and Ψ_{mn} may be defined in terms of quasi-particle occupation numbers of metals a and b, so that Ψ_{mn} differs from Ψ_0 in the transfer of an electron from state m in a to state n in b, all other occupation numbers remaining the same. Of course m may correspond to a normally occupied state, in which case there will be a hole in m in Ψ_{mn}.

The quasi-particles do not correspond to plane waves, but to waves which are reflected at the barrier and which drop exponentially with distance into the barrier region. For example, in the free-electron approximation for the normal state the wave function would be of the form (WKB approximation):

$$\psi_m = Cp_x^{-1/2} e^{i(p_y y + p_z z)} \sin(p_x x + \gamma), \quad x < x_a \tag{1a}$$

$$\psi_m = \tfrac{1}{2} C |p_x|^{-1/2} e^{i(p_y y + p_z z)} \times \exp\left(-\int_{x_a}^{x} |p_x| dx\right), \quad x_a < x < x_b \tag{1b}$$

where $C = (2p_x/L)^{1/2}$ is a normalization constant, and in the barrier region, $|p_x| = (2\mu U - p_y^2 - p_z^2)^{1/2}$, where $U(x)$ is the potential energy. We have taken units such that $\hbar = 1$. Beyond x_b, we assume that the wave function representing the electron in state m drops smoothly to zero, instead of oscillating, so that it is not a good solution for $x > x_b$.

Thus we assume that Ψ_0 is a solution of the Schrödinger equation with energy W_0 for $x < x_b$, but there is a region to the right of x_b where it is not a good solution. Similarly, we assume that Ψ_{mn} with energy W_{mn} is a solution for $x > x_a$, but not for the region to the left of x_a where the wave function for quasi-particle n drops to zero. Both Ψ_0 and Ψ_{mn} are good solutions in the barrier region $x_a < x < x_b$.

We form a time-dependent solution as a linear combination of Ψ_0 and various final states, Ψ_{mn}, by the usual method:

$$\Psi = a(t)\Psi_0 e^{-iW_0 t} + \sum_{mn} b_{mn}(t)\Psi_{mn} e^{-iW_{mn} t}, \tag{2}$$

and substitute into the Schrödinger equation. This gives for the matrix element for the transition

$$M_{mn} = \int \Psi_0^* (H - W_{mn}) \Psi_{mn} d\tau. \tag{3}$$

Since the integrand vanishes except over a region to the left of x_a, we need to integrate only over this region.

We may express the integral in a more symmetric form by subtracting $\Psi_{mn}(H - W_0)\Psi_0^*$, which vanishes to the left of x_b. Since we are interested only in final states such that $W_{mn} \simeq W_0$, the result may be written

$$M_{mn} = \int_a [\Psi_0^* H \Psi_{mn} - \Psi_{mn} H \Psi_0^*] d\tau, \tag{4}$$

where the subscript a indicates that the integration is to be taken over the region to the left of x_a.

The matrix element may be expressed in terms of that of the current density operator, J, in the barrier region as follows. We introduce into the integrand a step function $S(x)$ which is equal to unity between a point x_0 to the left of the important region of integration and a point x_1 in the barrier and which vanishes elsewhere. Then integrations with respect to y_i and z_i vanish and integration with respect to x_i gives

$$M_{mn} = -\frac{1}{2\mu} \sum_i \int \cdots \int (\Psi_0^* \nabla_i^2 \Psi_{mn} - \Psi_{mn} \nabla_i^2 \Psi_0^*) S(x_i) d\tau_1 \cdots d\tau_N$$

$$= -i[J_{mn}(x_1) - J_{mn}(x_0)], \tag{5}$$

where $J_{mn}(x)$ is the matrix element of the x component of the current density operator defined by

$$J_{mn}(x) = -\frac{i}{2\mu} \sum_i \int \cdots \int [\Psi_0^* \partial \Psi_{mn}/\partial x_i - \Psi_{mn} \partial \Psi_0^*/\partial x_i] \delta(x - x_i) d\tau_1 \cdots d\tau_N. \tag{6}$$

According to our assumptions, $J_{mn}(x_0)=0$ and further, $J_{mn}(x_1)$ is independent of position as long as x_1 is in the barrier region. Thus

$$M_{mn}=-iJ_{mn}(x_1). \tag{7}$$

It is easily verified that this method leads to the usual results for barrier penetration problems.

The quasi-particle energy in a superconductor is $E=(\epsilon^2+\Delta^2)^{1/2}$, where $\epsilon(k)$ is the normal state energy measured from the Fermi surface. In calculating the density of final states, it is simplest to take the conventions that $f=1$ and E is negative for the normally occupied states in the Fermi sea, so that for $k<k_F$, the probability of a hole excitation is $1-f$ and the energy of a hole is $-E$. This is the procedure which has been used in the interpretation of the experimental data.[1,2] In each region of k space the density of states in energy in the superconductor differs from that in the normal metal by the factor

$$\rho_s=\rho_n\left[|E|/(E^2-\Delta^2)^{1/2}\right], \tag{8}$$

with $\rho_S=0$ in the gap, $|E|<\Delta$. Agreement with experiment is obtained if it is assumed that M_{mn} (or J_{mn}) is the same for the corresponding transitions in normal and superconducting states.

Usually coherence factors, which have a marked effect on transition probabilities, are introduced in calculations of matrix elements between quasi-particle states of a superconductor.[3] To see why such factors are not expected to occur in tunnelling, one must consider the pairing in the vicinity of the barrier. Coherence factors would be introduced if one simply paired complex conjugate wave functions of the type (1a), (1b), so that pairing extends into the barrier region. However, if one looks at the problem more closely, from the viewpoint of the more general Gor'kov equations[4] which allow for a variation of the energy gap parameter with position, one sees that Δ will drop to zero very rapidly in the barrier. In effect electrons in this region are not paired and the wave function is essentially the same as in the normal state.

For an effective interaction $v(\vec{r}_1,\vec{r}_2)$, the position-dependent energy gap function is defined by

$$\Delta(\vec{r}_1,\vec{r}_2)=\langle N-2|\psi(\vec{r}_1)\psi(\vec{r}_2)|N\rangle_{\mathrm{av}}\, v(\vec{r}_1,\vec{r}_2). \tag{9}$$

Simply from the fact that ψ is very small in the barrier region, one expects that $\Delta(\vec{r}_1,\vec{r}_2)$ is small when either $\vec{r}_1$ or $\vec{r}_2$ is in the barrier. Note that the tail in the barrier of the wave function of a typical electron at the Fermi surface is very much smaller than that of one of the few electrons moving normal to the interface which has an appreciable probability of penetrating. However, $\Delta(\vec{r}_1,\vec{r}_2)$ is expected to rise very rapidly to normal values in the superconductor, $\Delta(\vec{r}_1,\vec{r}_2)\simeq\delta(\vec{r}_1-\vec{r}_2)\Delta$, with $\Delta=\text{const}$.

Since, according to (6), the matrix element depends only on the wave function in the barrier, it would be expected to be the same as for the corresponding transition in the normal state. Actually, the wave function in the barrier would be changed slightly because of the difference in quasi-particle energies in normal and superconducting states, but this would have a negligible effect on the matrix elements. Thus the only significant difference in the tunnelling current comes from the density of states factor.

The method described here can also be used for calculating the tunnelling current between the valence and conduction bands of a semiconductor, as observed in the Esaki diode. It can be generalized to take indirect transitions into account.

The author is indebted to Dr. W. A. Harrison and Dr. J. R. Schrieffer for discussions of the theory of tunnelling in a superconductor.

---

*This work was supported in part by the Office of Ordnance Research, U. S. Army.

[1]Ivar Giaever, Phys. Rev. Letters 5, 147, 464 (1960).

[2]J. Nicol, S. Shapiro, and P. H. Smith, Phys. Rev. Letters 5, 461 (1960).

[3]J. Bardeen, L. N. Cooper, and J. R. Schrieffer, Phys. Rev. 408, 1175 (1957).

[4]L. P. Gor'kov, J. Exptl. Theoret. Phys. U.S.S.R. 34, 735 (1958) [translation: Soviet Phys.-JETP 34(7), 505 (1958)].

ELECTRIC QUADRUPOLE SPLITTING AND THE NUCLEAR VOLUME EFFECT IN THE IONS OF Fe^{57}†

S. DeBenedetti, G. Lang, and R. Ingalls*
Carnegie Institute of Technology, Pittsburgh, Pennsylvania
(Received December 19, 1960)

A study of the Mössbauer spectra of Fe^{57} in chemical compounds has revealed some striking regularities. Typical transmission curves for Fe^{++} and Fe^{+++} ionic compounds relative to an unsplit room-temperature stainless steel source are shown in Figs. 1 and 2, respectively. Both patterns exhibit a shift of the center of gravity from the zero of velocity, and the curve of Fe^{++} shows the two absorption lines characteristic of a pure nuclear electric quadrupole interaction. The quantities δ and ΔE, which characterize these effects, are defined in the figures; their values for various compounds are shown in Table I. It is noteworthy that the value of δ and the low-temperature value of ΔE are, for a given iron ion, relatively independent of the chemical combination.

The center of gravity displacement, or chemical shift,[1] arises from two mechanisms: (a) the second order Doppler shift,[2,3] which is caused by lattice vibrations, and is a function $A(T_S, T_a, \theta_S, \theta_a)$ of the source and absorber temperatures and Debye temperatures, and (b) the nuclear volume effect,[4,5] which represents the change, from source to absorber, in the modification of the nuclear transition energy caused by electrons overlapping the finite nucleus. The total shift in a Mössbauer spectrum may be written:

$$\delta \approx A(T_s, T_a, \theta_s, \theta_a) + B(R_e^{2\rho} - R_g^{2\rho})[\Psi_a^2(0) - \Psi_s^2(0)], \quad (1)$$

where R_e and R_g are the charge radii of the nuclear excited and ground states. $\Psi^2(0)$ is the s-electron density at the position of the nucleus. B is a constant which is 1.76×10^9 cm/sec for iron when $R^{2\rho}$ and $\Psi^2(0)$ are expressed in atomic units. $\rho=(1-\alpha^2Z^2)^{1/2}$ is a relativistic factor[5] equal to 0.982 for iron.

An estimate of R_g/R_e may be made if one neglects the influence of the crystalline surroundings and uses wave functions[6] for the free iron ions. Using (1) and the room-temperature shifts (which are less sensitive to differences in θ than are the low-temperature shifts), we obtain

$$\delta_{++} - \delta_{+++} \approx B(R_e^{2\rho} - R_g^{2\rho})[\Psi_{++}^2(0) - \Psi_{+++}^2(0)]. \quad (2)$$

We have neglected the small difference $A_{++} - A_{+++}$. Watson's wave functions yield $\Psi_{++}^2(0) < \Psi_{+++}^2(0)$; the extra electron in Fe^{++} apparently shields the $3s$ electrons slightly. Equation (2) yields $R_g/R_e = 1.001$.

Watson[6,7] has also calculated wave functions for the outer electron configurations $3d^64s^2$ and $3d^6$ for iron. Using an equation similar to (2) one obtains the shifts expected for each case:

$$\delta_{Fe} = -0.178 \text{ cm/sec for } 3d^64s^2,$$

$$\delta_{Fe} = +0.182 \text{ cm/sec for } 3d^6.$$

When metallic iron is used as an absorber with the stainless steel source at room temperature, a shift of +0.01 cm/sec results. Since this value is midway between the above calculated values,

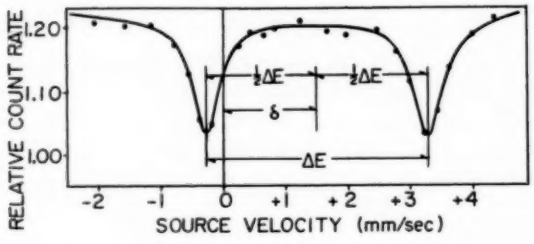

FIG. 1. Mössbauer spectrum of the Fe^{++} ion in an absorber of $FeSo_4\cdot7H_2O$ at nitrogen temperature using a room-temperature stainless steel source. The pattern exhibits the chemical shift δ and the electric quadrupole splitting ΔE of the excited state of the Fe^{57} nucleus. The velocity is positive for the source approaching the absorber.

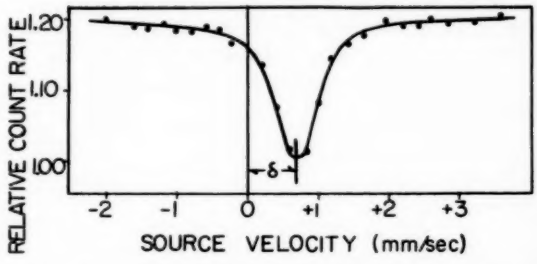

FIG. 2. Mössbauer spectrum of the Fe^{+++} ion in a $FeCl_3$ absorber at nitrogen temperature using a room-temperature stainless steel source. The velocity is positive for the source approaching the absorber.

Table I. A list of quadrupole splittings ΔE and chemical shifts δ relative to the emission line from a stainless steel source at room temperature.

Absorber	Temperature	ΔE(cm/sec)	δ(cm/sec)	References
Fe_2O_3	Room	0.024 ± 0.003	0.047 ± 0.003	a
Fe_2O_3	Room	0.024	0.050	b
$Fe_2(SO_4)_3$	Room	0	0.064	b
$Fe_2(SO_4)_3$	Room	0	0.055 ± 0.005	this work
$Fe_2(SO_4)_3$	Nitrogen	0	0.065 ± 0.005	this work
$FeCl_3$	Room	0	0.045 ± 0.005	this work
$FeCl_3$	Nitrogen	0	0.065 ± 0.005	this work
$FeCl_2 \cdot 4H_2O$	Room	0.300 ± 0.005	0.135 ± 0.005	this work
$FeCl_2 \cdot 4H_2O$	Nitrogen	0.310 ± 0.005	0.145 ± 0.005	this work
$FeSO_4 \cdot 7H_2O$	Room	0.320 ± 0.005	0.140 ± 0.005	this work
$FeSO_4 \cdot 7H_2O$	Nitrogen	0.360 ± 0.005	0.150 ± 0.005	this work
$Fe(NH_4)_2(SO_4)_2 \cdot 6H_2O$	Room	0.175 ± 0.005	0.140 ± 0.005	this work
$Fe(NH_4)_2(SO_4)_2 \cdot 6H_2O$	Nitrogen	0.270 ± 0.005	0.150 ± 0.005	this work
FeF_2	Room	0.268		c

[a]See reference 4.

[b]I. Solomon, Proceedings of the Allerton Park Conference on Mössbauer Effect, University of Illinois, Urbana, Illinois, June 5-7, 1960 (unpublished), Sec. IIc.

[c]G. K. Wertheim, Phys. Rev. 121, 63 (1961).

it strongly suggests that metallic iron has an outer electron configuration equivalent to $3d^7 4s^1$.

Although the electric quadrupole splitting seems to be temperature dependent, it is roughly the same at low temperatures for all the Fe^{++} compounds listed in Table I. This suggests that the relevant field gradient is mainly caused by the ion alone. The free Fe^{++} ion has an outer electron configuration of $3d^6$ and is in a ^5D state. Five of these $3d$ electrons have their spins aligned and together form a spherically symmetric distribution of charge. The sixth electron has opposite spin and also a choice of the five possible values of m_l. The crystal symmetry dictates the m_l combination the ion will actually take. For sufficiently low symmetry the lowest energy state will be a linear combination of the two states with m_l equal to 2 and -2. Assuming this, and neglecting all other possible effects of the crystalline environment, it is possible to calculate the ionic field gradient at the nucleus to within the factor $(1-\gamma)$, where γ is the Sternheimer antishielding factor. Taking ΔE to be 0.3 cm/sec one obtains $|Q(1-\gamma)| \approx 0.1$ b, where Q is the nuclear electric quadrupole moment for the excited state of Fe^{57}.

The temperature dependence of the quadrupole splitting could be caused by thermal excitation of the Fe^{++} ion into a state which yields a lower field gradient at the nucleus. For sufficiently rapid ionic transitions, the nucleus will respond to the time average of the field gradient. This interpretation indicates that the level splitting of the Fe^{++} ion in $Fe(NH_4)_2(SO_4)_2 \cdot 6H_2O$ is sufficiently small that significant excitation occurs at room temperature.

It is noted that there is very little quadrupole splitting in the case of Fe^{+++}. Presumably there is negligible field gradient from this ion, since its $3d^5$ electron configuration gives a ^6S state. The splitting that does occur[4] is therefore caused by field gradients from the neighboring ions rather than from the Fe^{+++} ion itself.

We are grateful to Professor J. Michael Radcliffe for some very helpful discussions.

†This work was supported by the Office of Naval Research.

*Submitted by R. Ingalls in partial fulfillment of the requirements for the degree of Doctor of Philosophy at the Carnegie Institute of Technology.

[1]O. C. Kistner, Proceedings of the Allerton Park Conference on Mössbauer Effect, University of Illinois, Urbana, Illinois, June 5-7, 1960 (unpublished), Sec. IIc.

[2]R. V. Pound and G. A. Rebka, Jr., Phys. Rev. Letters 4, 274 (1960).

[3]B. D. Josephson, Phys. Rev. Letters 4, 341 (1960).

[4]O. C. Kistner and A. W. Sunyar, Phys. Rev. Letters 4, 412 (1960).

[5]G. Breit, Revs. Modern Phys. 30, 507 (1958).

[6]R. E. Watson, Technical Report No. 12, Solid-State and Molecular Theory Group, Massachusetts Institute of Technology (unpublished).

[7]R. E. Watson, Phys. Rev. 119, 1934 (1960).

DETERMINATION OF THE PARITY CHANGE IN INELASTIC SCATTERING FROM THE ANGULAR DISTRIBUTION*

A. J. Kromminga and I. E. McCarthy
Department of Mathematical Physics, University of Adelaide, Adelaide, South Australia
(Received November 21, 1960)

Considerable success in determining the angular momentum transfer in direct-interaction inelastic scattering has been achieved by comparing the angular distribution in the approximate range 20° to 90° with $[j_L(KR)]^2$ or the improved theory due to Austern, Butler, and McManus.[1] Further information that one would like to obtain is the parity change of the nuclear state.

The distorted-wave Born approximation has been shown to give rather detailed fits to experimental data whether the final state is a single-particle[2] or collective[3] state. In a simplified distorted-wave Born approximation, Glendenning[4] found theoretical examples of angular distributions in which the forward differential cross section was very small for odd-parity change and very large for even-parity change. He suggested that this could be a general result which would make it possible to determine the parity change by a very simple experiment.

It is shown here in the distorted-wave Born approximation that, for reasonably small momentum transfers, the forward differential cross section is always small for odd-parity change and large for even-parity change. This result provides a very powerful tool for nuclear spectroscopy.

The matrix element for inelastic scattering in the distorted-wave Born approximation may be written

$$\mathfrak{M} \propto \int d^3r\, \varphi^{(+)}(\vec{k}, \vec{r})\varphi^{(-)*}(\vec{k}', \vec{r})\Psi(\vec{r}), \qquad (1)$$

where $\varphi^{(+)}$ and $\varphi^{(-)}$ are the wave functions of the incident and scattered particles whose momenta are $\hbar\vec{k}$ and $\hbar\vec{k}'$, respectively; $\Psi(\vec{r})$ contains all the properties of the initial and final nuclear states and the interaction. In the case of single-particle excitations,

$$\Psi(\vec{r}) = \int d^3r'\, \psi_i(\vec{r}')v(\vec{r}, \vec{r}')\psi_f^*(\vec{r}'), \qquad (2)$$

where ψ_i and ψ_f are the initial and final single-particle wave functions.

In the case of rotational excitations by spinless particles, in the notation of reference 3,

$$\Psi(\mathbf{r}) \propto \sum_\mu \langle v_f | Y_L^{\mu}(\theta_1, \theta_2) | v_i \rangle Y_L^{\mu *}(\Omega)(dU/dr), \qquad (3)$$

where θ_1, θ_2 are the orientation angles of the nucleus with respect to the space-fixed frame; Ω is the angular part of $\vec{r}$; v_f and v_i are the final and initial wave functions, respectively; and L is the orbital angular momentum change in the reaction.

The point is that the parity of $\Psi(\vec{r})$ in all cases, whether the incident and scattered particles have spin or not, is determined by the parities of the initial and final nuclear states; that is the parity change of the nucleus.

The remaining factor in $\Psi(\vec{r})$ has even parity including the pairs of spinor wave functions and spin-dependent interactions in the case where the scattered particles have spin.

The functions $\varphi^{(+)}$ and $\varphi^{(-)*}$ may be written

$$\varphi^{(+)}(\mathbf{r}) = \sum_l (2l+1) i^l \exp(i\sigma_l) R_l(kr) P_l(\cos\theta),$$

$$\varphi^{(-)*}(\mathbf{r}) = \sum_l (2l+1)(-i)^l \exp(i\sigma_l) R_l(k'r) P_l(\cos\theta'), \qquad (4)$$

where θ and θ' are measured from the direction of $\vec{k}$ and $\vec{k}'$, respectively.

Assuming that k and k' are not very different and that the optical model potentials seen by the incident and scattered particles are similar, we notice that, if the directions of $\vec{k}$ and $\vec{k}'$ are the same (forward scattering),

$$\varphi^{(+)}(\vec{r}) = \varphi(r, \pi - \theta),$$

$$\varphi^{(-)*}(\vec{r}) = \varphi(r, \pi - \theta).$$

Hence the product $\varphi^{(+)}(\vec{r})\,\varphi^{(-)*}(\vec{r})$ has approximately even parity.

If Ψ has odd parity (nuclear state undergoes parity change),

$$\mathfrak{M}(\vec{k}' \simeq \vec{k}) \simeq 0.$$

If Ψ has even parity (nuclear state undergoes no parity change),

$$\mathfrak{M}(\vec{k}' \simeq \vec{k}) \neq 0.$$

When $\varphi^{(+)}$ and $\varphi^{(-)*}$ are approximated by plane waves, the matrix element for forward scattering becomes

$$\mathfrak{M}(\vec{k}' \simeq \vec{k}) \propto \int_0^\infty r^2 dr \int_0^1 \exp(iKr\cos\theta) d(\cos\theta) \times \int_0^{2\pi} \Psi(\vec{r}) d\varphi, \tag{5}$$

where $\vec{K} = \vec{k} - \vec{k}'$. If the contribution from $L = 0$ to $\int \Psi(\vec{r}) d\varphi$ is small, then $\mathfrak{M}(\vec{k} \simeq \vec{k}) \simeq 0$.

When optical model wave functions are used for $\varphi^{(+)}$ and $\varphi^{(-)*}$, there is a strong θ dependence of the modulus of $\varphi^{(+)}$ and $\varphi^{(-)*}$. The integrand cannot be written in the form (5), since there is another θ-dependent factor. Hence if Ψ has even parity, $\mathfrak{M}(\vec{k} \simeq \vec{k})$ will not in general be small.

The θ dependence may be understood by considering $\varphi^{(+)}$. Let us write

$$\varphi^{(+)}(\vec{r}) = A_k(r, \theta)\, \exp[iS(r, \theta)]. \tag{6}$$

Then A_k decreases slowly as θ decreases from π, and, for nucleons of energy less than about 40 Mev, increases sharply as θ goes from about 15° to 0° (the focus). It has been shown[5] that the slow decrease from $\theta = \pi$ may be approximately absorbed into the factor $\exp(iKr\cos\theta)$ by making Kr complex. However, the focal contribution cannot be absorbed in this way and is responsible for the large value of $\mathfrak{M}(\vec{k}' \simeq \vec{k})$ when Ψ has even parity.

Glendenning's example suggests that, for nucleons of about 20 Mev, it would be possible to distinguish rising from falling differential cross sections by measurements down to 10°.

A crude estimate of the condition for the forward differential cross section to be small can be obtained from the approximation of reference 5 which has proved very successful in describing angular distributions in inelastic scattering of α particles:

$$\varphi^{(+)}(\vec{r}) = A_k(r, \theta)\, \exp(ikr\cos\theta),$$

$$\varphi^{(-)*}(\mathbf{r}) = A_{k'}(r, \pi - \theta)\, \exp(-ik'\cos\theta),$$

$$\mathfrak{M}(\vec{k}' \simeq \vec{k}) \propto \int d(\cos\theta)\, A_k(r_0, \theta) A_{k'}(r_0, \pi - \theta) \times \exp(iKr_0\cos\theta) \int d\varphi\, \Psi(\vec{r}_0). \tag{7}$$

Here we have restricted the radial integration to $r = r_0$.

The non-nuclear part of (7) is expected to have even parity if K is sufficiently small for the sine part of $\exp(iKr_0\cos\theta)$ to be always small compared to the cosine part. $\sin Kr_0 < 0.2$ for $r_0 = 5$ f if $K \lesssim 0.04$ f^{-1}. For 20-Mev neutrons, this corresponds to $|Q| \lesssim 1.6$ Mev. For higher energies $|Q|$ may be larger ($|Q|_{\max} \propto E^{1/2}$). This condition is easily satisfied by low-lying states of medium nuclei. Exact calculations should give a better idea of the range of applicability of the rule.

The result should apply also to reactions where the final and initial nuclei have the same mass such as (n,p) reactions, since the Coulomb potential does not severely modify the optical model wave functions in the interaction region.

---

*Supported in part by a Fulbright fellowship.

[1]N. Austern, S. T. Butler, and H. McManus, Phys. Rev. 92, 350 (1953).

[2]C. A. Levinson and M. K. Banerjee, Ann. Phys. 3, 67 (1958).

[3]E. Rost and N. Austern, in Proceedings of the International Conference on Nuclear Structure, Kingston, Canada, 1960, edited by D. A. Bromley and E. W. Vogt (University of Toronto Press, Toronto, 1960).

[4]N. K. Glendenning, Phys. Rev. 114, 1297 (1959).

[5]I. E. McCarthy and D. L. Pursey, in Proceedings of the International Conference on Nuclear Structure, Kingston, Canada, 1960, edited by D. A. Bromley and E. W. Vogt (University of Toronto Press, Toronto, 1960).

ROLE OF THE PERIPHERAL INTERACTION IN PROTON-PROTON COLLISIONS

Franco Selleri
CERN, Geneva, Switzerland
(Received December 19, 1960)

It has been suggested in a recent paper by Bonsignori and the writer[1] that the inelastic scattering of any particle on a target nucleon may be dominated by the exchange of one single virtual pion. Analyzing some known experiments,[2,3] it was there shown that in the Bev region there is good evidence for such a mechanism, when the incoming particle is a π meson or a nucleon. Further experiments[4] have shown the same qualitative evidence which consists essentially in a low-energy peaking of the laboratory spectrum of the recoil nucleon. It seemed therefore desirable to go further and calculate the cross section for the process

$$p+p\rightarrow p+n+\pi^{+} \qquad (1)$$

under the assumption of dominating peripheral interaction. We wish to stress that this dominance is assumed throughout the whole physical region and not only for very small momentum transfers as has been done in recent work.[5] The reason for choosing reaction (1) is that final-state interactions between the nucleons are negligible at high energy, while the (3, 3) interaction of the pion is likely to involve only one of the nucleons and thus not to destroy the typical effects of the one-pion exchange. A typical peripheral diagram for this process is shown in Fig. 1. p_1 and p_2 are the 4-momenta of the incoming protons; q, q_1, and q_2 those of the outgoing pion, proton, and neutron, respectively. Together with this, one should consider the other three diagrams obtained by exchanging the initial protons and the final nucleons.

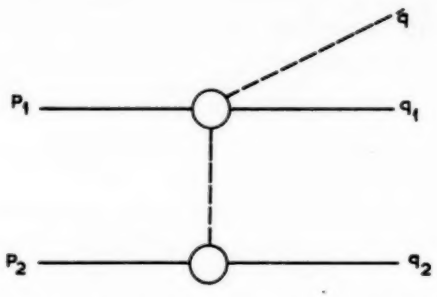

FIG. 1. Peripheral diagram contributing to process (1). Full and dashed lines represent nucleons and pions, respectively.

However, simple isotopic spin arguments show that the separate contribution to the total cross section for process (1) of the two diagrams in which the π^{+} and the neutron emerge from the same vertex is one ninth that of the diagram of Fig. 1. Therefore we can consider them of secondary importance and neglect them in our calculation. Furthermore, we shall be forced to calculate the nucleon-nucleon-pion vertex and the pion propagator to lowest order, and to substitute for the four-particle matrix element its expression known phenomenologically for the case in which all four particles are on the mass shell. We will see a posteriori upon comparison with experiments that these approximations probably are not too bad.

In the stated approximation the S-matrix element for process (1) can be written

$$S_{fi}=-(2\pi)^{7/2}\frac{m^{2}}{(2\omega_{q}E_{p_1}E_{p_2}E_{q_1}E_{q_2})^{1/2}}\delta^{4}(P_f-P_i)\sqrt{2}\,G_{\gamma}\frac{1}{\sqrt{2}}[M(p_1p_2)-M(p_2p_1)], \qquad (2)$$

where

$$M(p_1p_2)=\frac{\bar{u}(q_2)\gamma_5 u(p_2)}{(q_2-p_2)^{2}+\mu^{2}}\bar{u}(q_1)[-A+\hat{q}B]u(p_1). \qquad (3)$$

In (2), $\omega_q(E_l)$ is the zero component of the four-vector $q(l)$, $P_f=q+q_1+q_2$, $P_i=p_1+p_2$, and $\sqrt{2}\,G_{\gamma}$ is the rationalized and renormalized coupling constant for emission of a charged pion. The factor $2^{-1/2}$ and the minus sign are typical effects of the identity of the initial protons.[6] In (3), A and B are the well-known invariant amplitudes for pion-nucleon scattering (in our case in the state of isospin 3/2) as defined for example by Chew et al.,[7] and m (μ) is the nucleon (pion) mass. From (1) and (3) it is in principle possible to calculate any cross section at any energy. We choose to calculate $d\sigma/dT$, T being the lab kinetic energy of

the neutron. The importance of this variable was stressed in reference 1 and is essentially due to its simple relation with the 4-momentum transfer to the target nucleon: $(p_2 - q_2)^2 = 2mT$. In performing the actual calculation we had in mind a comparison with the 970-Mev experiment of the Birmingham group.[2] At this energy, the relative energies of the π^+ and the proton are in the region where the (3, 3) resonance dominates. We have therefore kept only the $J = 3/2$ P-wave part of A and B. For future reference we write down the result of our calculation:

$$\frac{d\sigma}{dT} = \frac{2f^2 m}{\pi p_i^2 \mu^2} \int_{m+\mu}^{g(T)} wR(w)\sigma(w)[a(T) + b(T, w) + c(T, w)]\,dw, \tag{4}$$

where $b^2 = \mu^2(16\pi m^2)^{-1} G_\gamma^2 = 0.08$, p_i is the lab momentum of the incoming proton, $w = [-(q + q_1)^2]^{1/2}$ is the total energy of π^+ and p in their c.m. system, and $\sigma(w)$ is the $\pi^+ p$ cross section at a c.m. energy w.[8] R, a, b, and c are the following functions:

$$R(w) = \tfrac{1}{2}[w^4 - 2w^2(m^2 + \mu^2) + (m^2 - \mu^2)^2]^{1/2}, \tag{5}$$

$$a(T) = \frac{\Delta_2^2}{(\Delta_2^2 + \mu^2)^2}, \tag{6}$$

$$b(T, w) = \frac{\Delta_1^2}{(\Delta_1^2 + \mu^2)^2}, \tag{7}$$

$$c(T, w) = \frac{\phi}{(\Delta_1^2 + \mu^2)(\Delta_2^2 + \mu^2)}, \tag{8}$$

$$\phi = (w - m)[(E_{p_2}' + m)(E_{p_1}' + m)]^{1/2} \cos\theta_i + (w + m)[(E_{p_2}' - m)(E_{p_1}' - m)]^{1/2} \frac{3\cos^2\theta_i - 1}{2}. \tag{9}$$

In the preceding formulas Δ_1^2 and Δ_2^2 are defined by

$$\Delta_1^2 = (p_2 - q_1)^2 = m^2 + 2m(T_i - T) - w^2,$$

$$\Delta_2^2 = (p_2 - q_2)^2 = 2mT,$$

T_i being the lab kinetic energy of the incoming proton and E_{p_1}', E_{p_2}', θ_i the energies of the initial protons and the angle between their directions, all in the c.m. system of the π^+ and the final proton. These three quantities can be expressed as a function of W, total c.m. energy for reaction (1), w^2, Δ_1^2, and Δ_2^2 through the following relations:

$$E_{p_1}' = (w^2 + m^2 + \Delta_2^2)/2w, \tag{10}$$

$$E_{p_2}' = (w^2 + m^2 + \Delta_1^2)/2w, \tag{11}$$

$$\cos\theta_i = (\vec{p}_1 \cdot \vec{p}_2)/p_1 p_2, \tag{12}$$

where $\vec{p}_1$ and $\vec{p}_2$ are three-momenta correspond-

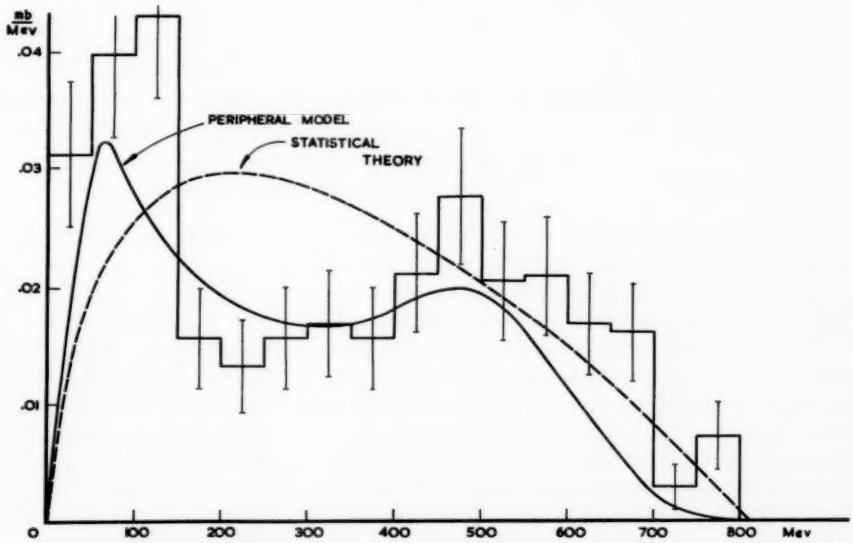

FIG. 2. Experimental energy spectrum in the lab system for neutrons from reaction (1) as compared with statistical theory (dashed line) and our formula (4) (full line).

ing to E_{p_1}' and E_{p_2}', respectively, and

$$\vec{p}_1 \cdot \vec{p}_2 = -\alpha + \frac{(2\alpha - \Delta_1^2)(2\alpha - \Delta_2^2)}{4\omega^2}, \qquad (13)$$

with $\alpha = W^2/2 - m^2$. Finally we have for the upper limit of integration

$$g(T) = \left[m^2 - W^2 \frac{T}{m} + W(W^2 - 4m^2)^{1/2} \left(\frac{T^2}{m^2} + \frac{2T}{m} \right)^{1/2} \right]^{1/2}. \qquad (14)$$

The predictions of formula (4) at 970 Mev are shown in Fig. 2 and compared with the experimental spectrum.[9] As is seen, the agreement is good while a statistical spectrum fails to explain the three main features of the experimental distribution; these are: the strong peaking at low (~50 Mev) energy, the broad bump at high (~500 Mev) energy, and the minimum between them. These features are, however, quantitatively predicted from our formula (4) and are typical effects of the peripheral interaction (see reference 1 for a more detailed discussion).

Theoretically, the total cross section[10] is predicted to be 12 mb; its experimental value is 16.4 ± 0.7 mb.[2] This indicates that something more than the diagrams of Fig. 1 contributes to process (1). However, this "something," whatever it is, is not more than 30% of the peripheral contribution. In view of these results it seems very desirable to have a deeper comparison between this model and the experimental data.[11]

The author is indebted to Professor A. Stanghellini and Dr. E. Ferrari for very useful suggestions, and also to many theoreticians of CERN for discussions.

[1]F. Bonsignori and F. Selleri, Nuovo cimento 15, 465 (1960).

[2]A. P. Batson et al., Proc. Roy. Soc. (London) 251, 218 (1959).

[3]V. Alles-Borelli et al., Nuovo cimento 14, 211 (1959).

[4]I. Derado, Nuovo cimento 15, 953 (1960); E. Pickup et al., Phys. Rev. Letters 5, 161 (1960).

[5]S. D. Drell, Phys. Rev. Letters 5, 278 (1960); 5, 342 (1960).

[6]N. N. Bogoliubov and D. V. Shirkov, Introduction to the Theory of Quantized Fields (Interscience Publishers, New York, 1959), p. 259.

[7]G. Chew et al., Phys. Rev. 106, 1337 (1957).

[8]In practical calculations one can use for $\sigma(w)$ either directly its experimental value or a phenomenological fit like the Breit-Wigner formula given by M. Gell-Mann and K. Watson, Annual Review of Nuclear Science (Annual Reviews, Inc., Palo Alto, California, 1954), Vol. 4, p. 219.

[9]This spectrum was already used in reference 1 and was originally a private communication from Dr. L. Riddiford to Professor A. Minguzzi.

[10]Calculations of the total cross section for process (1) under similar assumptions have already been performed by T. Kobayashi, Progr. Theoret. Phys. (Kyoto) 18, 318 (1957), who, however, did not take into account the effects of the Pauli principle, and by G. Da Prato, University of Rome, thesis (unpublished).

[11]This work was conceived as a collaboration with Professor A. Stanghellini, Dr. S. Bergia, and Dr. B. Bortolani of Bologna University who are now working on other aspects of the problem.

INTERMEDIATE BOSON PRODUCTION IN PION-PROTON COLLISIONS*

Norman Dombey
California Institute of Technology, Pasadena, California
(Received December 7, 1960)

The current-current hypothesis has been applied in recent years to the study of the weak interactions. The conserved vector current[1] hypothesis and the pionic character of the divergence of the axial vector current[2] have evolved in its wake. So has the idea of a boson field which mediates all weak interactions.[3] This note deals only with the vector part of the current, leaving for another time similar calculations with the axial vector part; and examines the possibility of producing the boson W, in pion-nucleon collisions, in case of W having relatively low mass.[4]

For definiteness let us consider the reaction

$$\pi^+ + p \rightarrow W^+ + p, \qquad (I)$$

and concentrate solely on the vector part of the interaction. Then, on inverting incoming and outgoing particles, it is apparent that the process is almost exactly the same as electroproduction of pions (i.e., production of pions by photons off the mass shell). The differences are: (*i*) The coupling constant is not the electromagnetic coupling constant. (*ii*) The four-momentum of the "photon" is timelike, not spacelike. But the anal-

ysis of electroproduction in papers A and B[5] is in fact relevant provided that instead of $e^2 = 1/137$, we write[3] $e^2 = (1/\pi\sqrt{2})(N^2/M^2)\times 10^{-5}$, where N is the boson mass and M is the proton mass. This simple substitution is the content of the conserved vector current hypothesis. The problems raised by (*ii*) imply the extrapolation of the analysis in A and B to a new region.

The total amplitude $\mathfrak{M}$ may be written in the form

$$\mathfrak{M} = AM_A + BM_B + CM_C + \cdots + FM_F, \qquad (1)$$

where the six functions A, B, $\cdots$, F depend on the invariants

$$\nu = -\frac{P\cdot k}{M}, \quad \nu_B = \frac{q\cdot k}{2M}, \quad k^2 = -N^2; \qquad (2)$$

here $P = \frac{1}{2}(p_1 + p_2)$; p_1, p_2 are the final and initial momenta of the proton; q, k the momenta of the π and W. M_A, $\cdots$, M_F are defined by Eq. (4) in A in terms of γ matrices. It is also possible to write $\mathfrak{M}$ in terms of two-component Pauli spin matrices:

$$\mathfrak{M} = \mathfrak{F} = \sum_{i=1}^{6} \Sigma_i \mathfrak{F}_i, \qquad (3)$$

where the Σ_i and the linear connection between the $\mathfrak{F}_i$ and the A, B, $\cdots$, F are given by Eqs. (8) and (9) in B. The cross section in the center-of-mass system is then given by

$$\frac{d\sigma}{d\Omega} = \frac{|\vec{k}|}{|\vec{q}|}\frac{M^2}{W^2}|\langle 2|\mathfrak{F}|1\rangle|^2, \qquad (4)$$

where W is the total energy in the c.m. system, and the matrix element includes the sum over final and average over initial spin states.

As the energy for reaction (I) is much above the 3-3 resonance of the pion-nucleon system, the calculation first will be done using only the Born terms. Here

$$A = -ef\,|F_1^p(k^2)|\left(\frac{1}{\nu_B - \nu} + \frac{1}{\nu_B + \nu}\right),$$

$$B = \frac{ef}{2M\nu_B}|F_1^p(k^2)|\left(\frac{1}{\nu_B - \nu} + \frac{1}{\nu_B + \nu}\right),$$

$$C = \mu_p' f\,|F_2^p(k^2)|\left(\frac{1}{\nu_B - \nu} - \frac{1}{\nu_B + \nu}\right),$$

$$D = \mu_p' f\,|F_2^p(k^2)|\left(\frac{1}{\nu_B - \nu} + \frac{1}{\nu_B + \nu}\right),$$

$$E = F = 0, \quad f^2 = 0.08, \quad \mu_p' = 1.78(e/2M); \qquad (5)$$

F_1^p and F_2^p are the Hofstadter form factors of the proton. Note that the form factors are of opposite sign in argument to those determined experimentally. The result of the calculations done with $F_1^p(k^2) = F_2^p(k^2) = 1$ for varying N at fixed energy is shown in Fig. 1. The cross section varies slowly with the energy for a given W mass.

It has been pointed out by Frazer and Fulco[6] that a π-π resonance in the state $I = 1$, $J = 1$ would give theoretical agreement with the experiments for the isotopic vector form factors. A more recent paper by Bowcock, Cottingham, and Lurié[7] fits the position and width of such a resonance to the data on π-N scattering and electromagnetic nucleon structure.

From the dispersion relations (with subtractions where necessary)

$$F_i^V(t) = \frac{1}{\pi}\int_{4\mu^2}^{\infty} \frac{g_i^V(t')dt'}{t' - t}, \quad (i = 1 \text{ or } 2) \qquad (6)$$

with

$$g_i^V(t') = |F_\pi(t')|^2[g_i^V(t')]_0, \qquad (7)$$

where the $[g_i^V(t')]_0$ are given in the papers on nucleon structure neglecting the π-π resonance,[8] the real and imaginary parts of $F_i^V(t = +N^2)$ can be calculated. The pionic form factor is given (for t not too large) by

$$|F_\pi(t)|^2 = \frac{t_\gamma^2}{(t - t_\gamma)^2 + \gamma^2 v^3}, \quad v = \tfrac{1}{4}t - \mu^2, \qquad (8)$$

when the π-π scattering amplitude is written in resonance form (for $I = 1$, $J = 1$)

$$f_{\pi\pi} = \frac{\gamma}{t_\gamma - t - i\gamma v^{3/2}}.$$

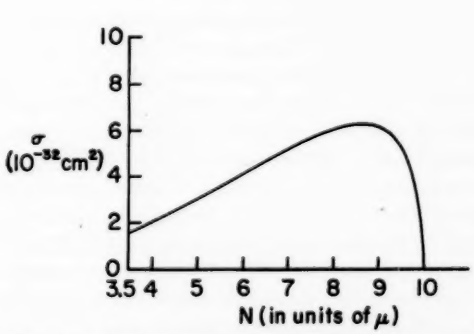

FIG. 1. Cross section σ as a function of boson mass N in uncorrected Born approximation. Momentum of pion in c.m. system is 980 Mev/c.

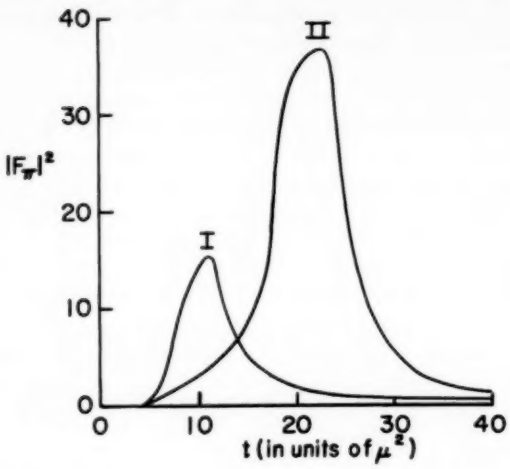

FIG. 2. Pionic form factor about resonance region. Curve I given by Frazer and Fulco. Curve II given by Bowcock, Cottingham, and Lurié.

In reference 7, the values for γ and t_γ are given as

$$\gamma = 0.376\mu^{-1}, \quad t_\gamma = 22.4\mu^2. \tag{9}$$

The two alternative curves for $|F_\pi(t)|^2$ are given in Fig. 2. The multiplicative factor (taking the charge and magnetic moment form factors to vary similarly in the low-energy unphysical region as well as the physical) to the curve in Fig. 1 is given in Table I.

An estimate of the effect of the 3-3 resonance was attempted using the dispersion relations for $A, \cdots, F$ given in A and B and replacing the resonance by a delta function, i.e.,

$$(1/\pi)\mathrm{Im}A(x) = A_{33}(x)\delta(1-\omega/\omega_\gamma), \text{ etc.,} \tag{10}$$

where $x = \nu - \nu_B$, $\omega = W - M$, ω_γ refers to the position of the resonance, and $A_{33}(x)$ is the 3-3 projection of the Born term for A, and is given in paper B. As the 3-3 resonance occurs well into the unphysical region for reaction (I), the amplitudes $A_{33}, \cdots, F_{33}$ must be analytically continued. If this is done and the calculation carried out for the total cross section, a very large increase is obtained (>100). There is no reason, however, to take this calculation seriously; but it should be viewed as an indication that the cross section may yet be larger than that given by the Born term with or without corrections.

Table I. Multiplicative factor given by π-π resonance to curve in Fig. 1 for various values of N.[a]

N	3.5	4	4.5	5	6	7	9
Frazer and Fulco	5	~1	~1	~1	<1	<1	<1
Bowcock, Cottingham, and Lurié	20	45	150	60	15	5	~1

[a] $F_i^S(N^2)$ is neglected.

So, in summing up, it can be said that if the Bowcock, Cottingham, and Lurié fit to the π-π resonance is correct, then the cross section should be of the order of 10^{-30} cm^2 for values of the W mass between four and five pion masses. It is also possible, if the 3-3 resonance is taken into account, that the cross section is greater still; and it must be remembered that the axial vector contribution has been completely neglected.

I would like to thank Dr. Leon Landovitz for suggesting this problem, Dr. G. C. Wick for his hospitality at Brookhaven National Laboratory, and Dr. Murray Gell-Mann and Dr. Fredrik Zachariasen for comments and advice.

---

*This work was begun at Brookhaven National Laboratory, Upton, New York.

[1]R. P. Feynman and M. Gell-Mann, Phys. Rev. 109, 193 (1958).

[2]J. Bernstein, S. Fubini, M. Gell-Mann, and W. Thirring, Nuovo cimento 17, 757 (1960).

[3]T. D. Lee and C. N. Yang, Phys. Rev. 119, 1410 (1960).

[4]It appears that the recently determined negative sign of the asymmetry parameter in Λ decay may require that W has a mass lower than two nucleon masses. J. C. Pati (private communication).

[5]S. Fubini, Y. Nambu, and V. Wataghin, Phys. Rev. 111, 329 (1958), Paper A; R. Blankenbecler, S. Gartenhaus, R. Huff, and Y. Nambu, Nuovo cimento 17, 775 (1960), Paper B.

[6]W. R. Frazer and J. R. Fulco, Phys. Rev. 117, 1609 (1960).

[7]J. Bowcock, W. N. Cottingham, and D. Lurié, Phys. Rev. Letters 5, 386 (1960).

[8]G. F. Chew, R. Karplus, S. Gasiorowicz, and F. Zachariasen, Phys. Rev. 110, 265 (1958); P. Federbush, M. L. Goldberger, and S. B. Treiman, Phys. Rev. 112, 642 (1958).

BINDING ENERGY OF THE TRITON

G. Derrick
University of Manitoba, Winnipeg, Canada

and

D. Mustard and J. M. Blatt,
New York University, New York, New York and the University of New South Wales, Sydney, Australia

(Received December 9, 1960)

We have made a variational calculation of the binding energy of the triton, using the same two-body nuclear force law which was used by Brueckner and Gammel in their calculation of the properties of nuclear matter,[1] and assuming, as they did, that there are no specifically many-body forces. Our results disagree with the experimental data on the binding energy of the triton and on the Coulomb radius of He^3, thereby excluding the Brueckner-Gammel force law.

Of the 10 different states which contribute to the ground-state wave function of the triton,[2] we have included 8. The two states omitted have fully antisymmetric "internal" wave functions (states Nos. 2 and 5 of reference 2), and thus high kinetic energy.

The trial wave functions were chosen as follows. For each state i ($i = 1, 2, \ldots, 10$), let

$$y_i \equiv \exp[-\gamma_i(r - r_0)], \tag{1}$$

where r_0 is the core radius, and γ_i is an adjustable parameter. Let a_{i3}, a_{i5}, a_{i7} be further parameters, and let

$$u_i(r) = \frac{1}{r}[y_i + a_{i3}(y_i)^3 + a_{i5}(y_i)^5 + a_{i7}(y_i)^7 - (1 + a_{i3} + a_{i5} + a_{i7})(y_i)^9]. \tag{2}$$

Then the trial wave function for the dominant, symmetric, $^2S_{1/2}$ state has the form

$$\psi_1 = A_1 u_1(r_{12}) u_1(r_{23}) u_1(r_{31}) + \bar{A}_1 \bar{u}_1(r_{12}) \bar{u}_1(r_{23}) \bar{u}_1(r_{31}), \tag{3}$$

where A_1, $\bar{A}_1$ are parameters, and $\bar{u}_1(r)$ differs from $u_1(r)$ only through the parameter values $\bar{\gamma}_1$, $\bar{a}_{13}$, $\bar{a}_{15}$, $\bar{a}_{17}$.

Wave functions of "mixed" symmetry, e.g., the mixed-symmetry $^2S_{1/2}$ state (state 3 of reference 2) are constructed as follows: Let

$$z_i = \exp[-2\delta_i(r - r_0)], \tag{4}$$

where δ_i is a parameter, let a_{i4}, a_{i6}, and a_{i8} be additional parameters, and let

$$v_i(r) = \frac{1}{r}[z_i + a_{i4}(z_i)^2 + a_{i6}(z_i)^3 + a_{i8}(z_i)^4 - (1 + a_{i4} + a_{i6} + a_{i8})(z_i)^5]. \tag{5}$$

Then the internal part of the final wave function for the mixed-symmetry $^2S_{1/2}$ state has the two components

$$\psi_{3,1} = A_3(3)^{-1/2}\{u_3(r_{12})[v_3(r_{23})u_3(r_{31}) + u_3(r_{23})v_3(r_{31})] - 2v_3(r_{12})u_3(r_{23})u_3(r_{31})\},$$

$$\psi_{3,2} = A_3 u_3(r_{12})[v_3(r_{23})u_3(r_{31}) - u_3(r_{23})v_3(r_{31})]. \tag{9}$$

Trial functions for P states and D states are constructed in an analogous fashion, with the appropriate factors in front so as to give the correct dependence on Euler angles and spins and the correct asymptotic behavior in the singular configurations (equilateral triangle, and triangle degenerating into a straight line).[3] However, the doubling-up of wave functions for one state, as in (3), is employed only for the dominant $^2S_{1/2}$ state, not for any other states.

The matrix elements of the Hamiltonian, using these states, involve sums over spin and isospin indices, integrals over Euler angles, and integrals over r_{12}, r_{23}, r_{31}. The spin sums and Euler angle integrations are done analytically,[3,4] the integrations over r_{12}, r_{23}, r_{31} numerically.[5] Depending upon the fineness of the net and upon the number of states used, the numerical integrations take between 10 minutes and 1 hour on the IBM 704. The number of netpoints ranges between 9000 and 30 000, and the upper limit on r_i between $R = 6.4\times10^{-13}$ cm and $R = 9.6\times10^{-13}$ cm. The dominant $^2S_{1/2}$ state integrals are done with a much finer net which gives 5-figure accuracy; the other integrals have numerical errors of the order of 1%. The numerical error in the expectation value of the Hamiltonian is estimated to be less than 0.3 Mev.

After varying some 40 parameters, we find for the ground-state energy of the triton

$$E_0 < -10 \text{ Mev}, \tag{7}$$

and for the Coulomb radius

$$R_c = 3.2\times10^{-13} \text{ cm}. \quad (8)$$

These values disagree with the experimental values, -8.49 Mev and 2.26×10^{-13} cm, respectively. Since this is a conventional variation calculation, any improvement in the wave function would increase the disagreement in the energy.

We do not believe that the upper bound (7) for E_0 is close to the mathematically correct ground-state energy. Every time we varied new parameters, or revaried ones varied much earlier, the bound on E_0 decreased another few tenths of an Mev. We merely quit varying parameters when the discrepancy with experiment became sufficiently large to be significant.

The D-state probability is about 7%; no direct comparison with experiment is possible for this quantity.

The P states are completely unimportant. States 4, 6, and 7 of reference 2 have probabilities 3.8×10^{-4}, 0.8×10^{-4}, and 1.9×10^{-4}, respectively, adding up to a total P-state probability of 6.5×10^{-4}. The contribution of the P states to the binding energy is less than 100 kev.

The $\vec{L}\cdot\vec{S}$ force contributes significantly, but not through the P states. Rather, the matrix elements of the $\vec{L}\cdot\vec{S}$ force between the D states must be included in the calculation, and these matrix elements contribute several Mev, in a repulsive direction.

The sharp variation of the trial functions near the core radius, especially for state 8 of reference 2, requires a reasonably fine net for the numerical quadratures.

The large number of states required, and the sensitivity of the result to the values of many of the parameters in each state, makes it appear doubtful that any simple approximation can give accurate results in a three-body problem with tensor forces. By analogy, simple approximations in the many-body problem may well turn out to be less accurate than supposed.

We conclude that the combination of the Gammel-Brueckner potential with the assumption of superposition of 2-body forces, is inconsistent with experimental data on the triton and He^3. This does not necessarily contradict the result of reference 1, since one and the same potential may disagree with H^3 and He^3 and yet agree with nuclear matter. However, it is not impossible that the accuracy of the Brueckner theory of nuclear matter is somewhat less good than had been hoped.

We are very grateful to the U. S. Atomic Energy Commission and the Institute of Mathematical Sciences, New York University, for travel allowances and a very generous allocation of machine time, which alone made this calculation possible. We greatly appreciate many helpful and informative discussions with Professor R. D. Richtmyer, Professor E. Isaacson, Professor Max Goldstein, and Mrs. B. Weitzenhoffer, and the unstinting and generous help given to us by them and by all the members of the staff of the Atomic Energy Commission Computing Center at New York University.

[1]K. A. Brueckner and J. L. Gammel, Phys. Rev. 109, 1023 (1958).

[2]G. Derrick and J. M. Blatt, Nuclear Phys. 8, 310 (1958); G. Derrick, Ph.D. thesis, Sydney University, 1959 (unpublished).

[3]G. Derrick, Nuclear Phys. 16, 405 (1960).

[4]G. Derrick, Nuclear Phys. 18, 303 (1960).

[5]J. M. Blatt and D. Mustard, Mathematics of Computation (to be published).

THE REACTION $\gamma+\gamma\rightarrow\nu+\bar{\nu}$[†]

Murray Gell-Mann
California Institute of Technology, Pasadena, California
(Received December 21, 1960)

In a current-current picture of the weak interactions, a coupling term of the form $(e\nu)(e\nu)$ arises.[1,2] The contribution from charge-exchange currents is an interaction Lagrangian

$$\frac{G}{\sqrt{2}}[\bar{e}\gamma_\alpha(1+\gamma_5)\nu][\bar{e}\gamma_\alpha(1+\gamma_5)\nu]^+, \quad (1)$$

in the case of local coupling. [If there are charge-retention currents involving leptons, other terms may occur, of course, conceivably even cancelling (1).]

In reference 2, the cross section for neutrino-electron scattering is calculated using the interaction (1); the result is too small for an experi-

mental test to have been possible up to the present time.

Pontecorvo[3] has suggested that if the coupling (1) exists, it may be of astrophysical importance because it would induce reactions leading to energy loss in stars. Recently[4] consideration has been given to processes like

$$e^- + e^+ \rightarrow \nu + \bar{\nu}, \tag{2}$$

which is similar to electron-neutrino scattering, and

$$\gamma + \gamma \rightarrow \nu + \bar{\nu}. \tag{3}$$

It is interesting that the latter process is not, in fact, induced by the local coupling (1). The reasoning is as follows:

By a Fierz transformation, we may express the coupling as

$$\frac{G}{\sqrt{2}}[\bar{e}\gamma_\alpha(1+\gamma_5)e][\bar{\nu}\gamma_\alpha(1+\gamma_5)\nu], \tag{4}$$

and we must then calculate the matrix element of $\bar{e}\gamma_\alpha e$ and of $\bar{e}\gamma_\alpha\gamma_5 e$ between the vacuum and a state of two photons. The first vanishes by charge conjugation invariance. The second is analogous to the amplitude for the decay of a pseudovector or a pseudoscalar meson into two photons. Since a spin 1 meson cannot decay[5] into two photons, only that part of the amplitude corresponding to a pseudoscalar meson survives. In the rest frame, only the time component can contribute. Thus the entire matrix element of $\bar{e}\gamma_\alpha(1+\gamma_5)e$ is equal to P_α (the total four-momentum) times a pseudoscalar bilinear in the field strengths of the two photons. But the Dirac equation for the neutrinos tells us that $\bar{\nu}P_\alpha\gamma_\alpha(1+\gamma_5)\nu$ gives zero.

Thus local weak interactions, to lowest order in G, give a vanishing rate[6] for reaction (3). Our proof does not hold, however, for the case of an intermediate charged vector boson[2] mediating the charge-exchange current-current interactions. That case must be investigated further.

The process[4] $\gamma + \gamma \rightarrow \nu + \bar{\nu} + \gamma$ is not forbidden for local coupling, although the contribution from $\bar{e}\gamma_\alpha\gamma_5 e$ vanishes by charge conjugation symmetry. The remaining amplitude, coming from $\bar{e}\gamma_\alpha e$, can be calculated from the amplitude[7] for the corresponding process where the neutrino pair is replaced by a virtual photon with "field strength" equal to the matrix element of

$$\frac{G}{e\sqrt{2}}\left\{\frac{\partial}{\partial x_\alpha}[\bar{\nu}\gamma_\beta(1+\gamma_5)\nu] - \frac{\partial}{\partial x_\beta}[\bar{\nu}\gamma_\alpha(1+\gamma_5)\nu]\right\}$$

for creation of the neutrino pair.

The author wishes to thank Professor William A. Fowler and Mr. M. Levine for suggesting a study of the reactions discussed here.

---

†Supported in part by the Alfred P. Sloan Foundation.

[1]M. Gell-Mann and A. H. Rosenfeld, Annual Review of Nuclear Science (Annual Reviews, Inc., Palo Alto, California, 1957), Vol. 7, p. 407.

[2]R. P. Feynman and M. Gell-Mann, Phys. Rev. 109, 193 (1958).

[3]B. Pontecorvo, J. Exptl. Theoret. Phys. (U.S.S.R.) 36, 1615 (1959) [translation: Soviet Phys.-JETP 9, 1148 (1959)].

[4]See, for example, H.-Y. Chiu and P. Morrison (to be published).

[5]C. N. Yang, Phys. Rev. 77, 242 (1950).

[6]It should be noted that the important process γ + Coulomb field $\rightarrow \nu + \bar{\nu}$ does occur in the case of local coupling. In the lowest order of perturbation theory, the gauge-invariant amplitude for this reaction is finite and calculable.

[7]R. Karplus and M. Neuman, Phys. Rev. 80, 382 (1960).

ABSTRACTS

In this section are printed the abstracts of Articles that have been forwarded to The American Institute of Physics for publication in THE PHYSICAL REVIEW. In quoting information obtained from this section before the appearance of the corresponding Article, reference should be made to "Physical Review (to be published)" rather than to this Journal.

THE DIFFERENCE IN THE MULTIPLE SCATTERING OF ELECTRONS AND POSITRONS. B. P. Nigam, Department of Physics and Astronomy, University of Rochester and The Research Division, Stromberg-Carlson, a Division of General Dynamics, Rochester, New York and V. S. Mathur, The Enrico Fermi Institute for Nuclear Studies, University of Chicago, Chicago, Illinois (Received November 9, 1960).

The difference in the multiple scattering of electrons and positrons has been calculated on the basis of the work of Nigam, Sundaresan, and Wu. The results are compared with the experimental work of Henderson and Scott and are found to be in good agreement.

FREQUENCY FACTORS IN THE THERMALLY ACTIVATED PROCESS. R. Landauer and J. A. Swanson,* International Business Machines Research Center, Yorktown Heights, New York (Received November 3, 1960).

Discussions of the rate, $\nu e^{-U/kT}$, for thermally activated processes, are usually based on the phase-space distribution function for thermal equilibrium. Kramers has gone beyond this and for the particle in a bistable one-dimensional well has treated the relaxation to equilibrium as a Brownian motion problem in which the one-dimensional motion is coupled to a reservoir through a viscosity. Kramers' arguments are readily extendable to many dimensions. In the overdamped case the reaction rate is reduced below the value derived from thermal equilibrium theory by the factor ω_S/η, where ω_S is the angular frequency associated with the direction of steepest descent at the saddle point and η is the viscosity. In the underdamped case equilibrium theory is valid for many-dimensional systems, except for extreme degrees of underdamping.

*Deceased.

DIELECTRIC RELAXATION DUE TO IMPURITY-VACANCY COMPLEXES IN NaCl CRYSTALS. R. W. Dreyfus, International Business Machines Research Center, Yorktown Heights, New York (Received September 19, 1960; revised manuscript received December 5, 1960).

Sodium-ion vacancies are introduced into sodium chloride crystals by the addition of the following divalent cation impurities: Mg^{++}, Mn^{++}, Ca^{++}, Zn^{++}, Cd^{++}, and Sr^{++}. Below 150°C, the virtual negative charge of a cation vacancy binds the majority of the vacancies to the divalent impurity ions to form complexes. The reorientation of these dipolar complexes is observed in the present experiments as a transient dielectric polarization current occurring immediately after the application of a dc electric field. Below 0°C, the current is made up of an initial exponential "fast polarization" due to complexes in which the vacancy is in the nearest sodium-ion site to the impurity ion, plus a "slow polarization" ascribed to vacancies jumping between more distant bound sites. The results for NaCl:Mn^{++} crystals show that relaxation of vacancies which are nearest neighbors to the Mn^{++} ion, occurs with an activation energy of 0.680 ± 0.010 ev. From the manner in which the relaxation time at a given temperature varies with the radius of the impurity ion, the dominant jump mechanisms can be inferred. The major reason for the decrease in relaxation time with decreasing radius of the impurity ion appears to be the strong dependence of the jump rate of the impurity ion on ionic radius.

EFFECTS OF APPLIED ELECTRIC FIELDS ON PARAMAGNETIC RESONANCE IN CHROME ALUMS. M. E. Browne, Lockheed Research Laboratories, Palo Alto, California (Received October 3, 1960; revised manuscript received December 7, 1960).

The paramagnetic resonance spectra of single crystals of potassium chrome alum and ammonium chrome alum have been investigated in the presence of applied electric fields at 9.3 kMc/sec in the temperature range 4-300°K. The measurements were made in an effort to detect the possible existence of a term of the form $\xi\mu_0\vec{\sigma}\cdot\vec{\vec{E}}$ in the interaction Hamiltonian for an electron in an electromagnetic field. Such a term corresponds to the existence of an electron electric dipole moment and would result in a lifting of Kramers' degeneracy for a magnetic ion in a crystalline

field. No such term was observed, and the upper limit on ξ obtained was $\xi < 0.007$. A dependence of the dielectric loss on electric field was observed in both alums at microwave frequencies.

ORDER-DISORDER MODEL THEORY FOR THE FERROELECTRIC EFFECT IN THE DIHYDROGEN PHOSPHATES. Michael E. Senko, International Business Machines Research Center, Yorktown Heights, New York (Received November 7, 1960).

A term in polarization energy is added to the Slater-Takagi model of ferroelectricity in $KH_2PO_4(KDP_H)$. This free-energy function relates the shift in Curie point temperature due to deuteration of the compound with the measured change in saturation spontaneous polarization. The dielectric constant, ϵ_C, obtained by numerical differentiation of the free-energy function has a sharp maximum at the Curie temperature. With a change of parameters, the model also reproduces some of the details of antiferroelectric behavior.

ISOTOPE EFFECT IN INTERMETALLIC DIFFUSION. James G. Mullen,* Physics Department, University of Illinois, Urbana, Illinois (Received November 7, 1960).

Ten measurements of the isotope effect for diffusion of Fe^{55} and Fe^{59} in pure single crystals of silver and copper have been made over approximately a 300-C° temperature interval below the melting point. The measured isotope effect was found to be about 2/3, significantly less than the value of unity expected from conventional reaction rate theory.

It is shown from Vineyard's extension of reaction rate theory that the measured isotope effect is to a good approximation a product of the Bardeen-Herring correlation factor and the fraction of the total translational kinetic energy associated with the diffusing tracer in a tracer-vacancy exchange. It is shown that the ring, interstitialcy, crowdion, and relaxation mechanisms are not responsible for diffusion in the systems studied.

The three-frequency theory of correlation for vacancy diffusion in fcc lattices is extended to show that the relative frequency factors are completely specified by a knowledge of the correlation factor and the diffusion coefficients. An expression for the difference in the Arrhenius Q and the activation energy due to the temperature dependence of the correlation factor is derived. This theory is shown to be inconsistent with the observed isotope effect if many-body effects are neglected. It is shown that a "long-range" repulsive interaction between the vacancy and impurity would be necessary if the measured isotope effect is to be explained purely in terms of correlation.

*Present address: Solid-State Science Division, Argonne National Laboratory, Argonne, Illinois.

ELASTIC CONSTANTS OF AMMONIUM DIHYDROGEN PHOSPHATE (ADP) AND THE LAVAL THEORY OF CRYSTAL ELASTICITY. Hans Jaffe, Clevite Corporation, Cleveland, Ohio and Charles S. Smith, Case Institute of Technology, Cleveland, Ohio (Received November 14, 1960).

The acoustic shear wave velocities v_{yz} and v_{zy} have been measured in ADP by the direct method of piezoelectric resonances, and by the direct pulse echo method. These velocities are found with each method to be equal within the experimental uncertainty. The resonance results have a probable error of 0.1% for the difference between the corresponding Laval elastic constants c_{44} and c_{77}. This experimental result disagrees with those previously obtained with ADP by indirect methods.

PROTON MAGNETIC RESONANCE STUDY OF POLYCRYSTALLINE $HCrO_2$. James A. Ibers, C. H. Holm, and C. R. Adams, Shell Development Company, Emeryville, California (Received October 21, 1960).

A proton magnetic resonance study of polycrystalline $HCrO_2$ as a function of magnetic field and temperature is presented. $HCrO_2$ is paramagnetic, and electron paramagnetic dipole as well as nuclear dipole effects lead to line broadening. The lines are asymmetric, and over the range of field $470 \leq H_0 \leq 9400$ gauss and temperature $77° \leq T \leq 294°K$ the asymmetry increases with increasing H_0 and decreasing T. An isotropic resonance shift of 0.017% to lower applied fields indicates a weak isotropic hyperfine contact interaction. The general theory of resonance

shifts is used to derive a general expression for the second moment M_{2p} of a polycrystalline paramagnetic sample and is specialized to $HCrO_2$. The theory predicts a linear dependence of M_{2p} on $[H_0/(T+\theta)]^2$, where θ is the experimentally determined Curie-Weiss constant. The experimental second moment M_{2p}' conforms to the relation

$$M_{2p}' = (3.96 \pm 0.06) + (0.084 \pm 0.002)[H_0/(T+276)]^2,$$

in agreement with theory. Hence the electron paramagnetic effects (slope) can be separated from the nuclear effects (intercept). The paramagnetic dipole effects provide some information on the particle shapes. The nuclear dipole effects provide some information on the motions of the hydrogen nuclei, but the symmetry of the O-H-O bond in $HCrO_2$ remains in doubt.

OBSERVATIONS OF ELECTRON-HOLE CURRENT PINCHING IN INDIUM ANTIMONIDE. M. Glicksman and R. A. Powlus, RCA Laboratories, Princeton, New Jersey (Received November 8, 1960).

The temporal variation at high electric fields of the current and voltage in n-type InSb is examined. The observations show the behavior characteristic of self-pinching of the electron-hole plasma current. There is good agreement with theory for the observed times for the pinching process as a function of current. The calculated sum of the average energies of the electrons and holes in the plasma is 0.037 ev. Oscillations in the electric field of apparently different character are observed during the pinch, and when a longitudinal magnetic field is applied.

EFFECTS OF A MAGNETIC FIELD ON HEAT CONDUCTION IN SOME FERRIMAGNETIC CRYSTALS. D. Douthett* and S. A. Friedberg, Carnegie Institute of Technology, Pittsburgh, Pennsylvania (Received November 10, 1960).

The thermal conductivities of single-crystal bars of several ferrites have been measured over the temperature range 1.4° to 25°K both in zero external magnetic field and in a field of about 9.4 kilo-oersteds. For each specimen the zero-field conductivity is a smooth function of the temperature over the entire range considered. The magnitudes of the conductivities of the manganese and cobalt-zinc ferrite specimens are quite low, approximately 1.5 mw/cm-°K at 4°K. Upon application of a magnetic field parallel to the direction of heat current flow, the conductivities of the manganese ferrite and cobalt-zinc ferrite specimens are increased. The magneto-conductivities are rather large. For example, $\Delta K/K_0 = 0.2$ for manganese ferrite at 2°K. Such a field produces no detectable change in the conductivity of the manganese-zinc ferrite. The experimental results are interpreted on the basis of the assumption that the heat current is primarily a phonon current limited by phonon-magnon scattering.

*Presently with Ramo-Wooldridge Research Laboratory, Canoga Park, California.

SUPERCONDUCTING TRANSITION IN ZINC AND GALLIUM. John F. Cochran* and D. E. Mapother, Physics Department, University of Illinois, Urbana, Illinois (Received November 14, 1960).

The superconducting transitions of Ga and Zn have been studied to compare the supercooling of these elements with that shown by Al under similar conditions. Both Ga and Zn show considerably less tendency to supercool than Al despite their lower critical temperatures. The measurements also provide values of T_c and $(dH_c/dT)_{T_c}$ for Ga and Zn for comparison with recently reported calorimetric data. Attention is called to the fact that discrepancies still exist between direct calorimetric determination of the specific heat discontinuity at the critical temperature and the value deduced thermodynamically from critical-field data. It is shown that such discrepancies are conspicuously worse among the elements Zn, Ga, and Al than for the elements of higher T_c (In, Sn, Ta, and Pb) where agreement is within experimental error.

*Present address: Physics Department, Massachusetts Institute of Technology, Cambridge, Massachusetts.

NUCLEAR QUADRUPOLE ABSORPTION IN INDIUM METAL. W. W. Simmons* and C. P. Slichter, Department of Physics, University of Illinois, Urbana, Illinois (Received November 7, 1960).

The nuclear quadrupole resonance spectrum of indium metal has been observed and studied over the temperature range 4°K to 225°K. The four transition frequencies occur in ratios of

1:2:3:4, as expected from the crystal structure of indium. The lowest transition at 1.881 Mc/sec (at 4.2°K) gives a quadrupole coupling constant of (45.19 ± 0.02) Mc/sec.

The root second moment of 18 kc/sec is substantially greater than the 4 kc/sec predicted from magnetic dipolar coupling among the nuclei, is temperature independent, but somewhat sample dependent. It is shown that for a pure quadrupole resonance, the pseudoexchange coupling produces an exchange broadening. This mechanism is shown to contribute about 10 kc/sec to the root second moment and predicts a Gaussian line shape, as observed. It is concluded that in some cases magnetic impurities must be present, but it is not known whether or not the narrowest line represents a natural width.

The field gradient is computed assuming point ions and a uniform electron density by a technique that converges rapidly with distance, but the answer is too small by a factor of 3. It is argued that it is important to consider the p valence electrons. The temperature dependence of frequency is very strong (a 23% decrease between 4°K and 220°K), and unexplained. It appears to show that the field gradients cannot be computed assuming point ions and a smooth charge distribution.

A resonance in the superconducting state is reported.

*Now at Space Technology Laboratories, Inc., Los Angeles, California.

PARAMAGNETIC RESONANCE HYPERFINE STRUCTURE OF TETRAVALENT Pa^{231} IN Cs_2ZrCl_6. J. D. Axe, Department of Chemistry and Lawrence Radiation Laboratory, University of California, Berkeley, California, and H. J. Stapleton and C. D. Jeffries, Physics Department, University of California, Berkeley, California (Received November 7, 1960).

Paramagnetic resonance absorption at 3-cm wavelengths is observed for tetravalent Pa^{231} in a single crystal of Cs_2ZrCl_6 at helium temperatures. The observed spectra correspond to the allowed transitions $(S_z,\ I_z \rightarrow S_z \pm 1,\ I_z)$ and the forbidden transitions $(S_z,\ I_z \rightarrow S_z \pm 1,\ I_z \mp 1)$ of a system described by the spin Hamiltonian $H_S = g\beta\vec{H}\cdot\vec{S} + A\vec{I}\cdot\vec{S} - g_n'\beta\vec{H}\cdot\vec{I}$, with $S = 1/2$, $I = 3/2$, $|A|/h = 1578.6 \pm 1.4$ Mc/sec, $|g| = 1.1423 \pm 0.0014$, and $|g_n'| \approx 8\times10^{-4}$. The errors indicate a small deviation from isotropy. It is further observed that $g_n'/g < 0$, indicating that if g_n' is positive, as is strongly indicated by the nuclear shell model, then g is negative. An additional electron-nuclear double resonance experiment is used to determine directly the nuclear magnetic moment $\mu(Pa^{231}) = 1.96$ nuclear magnetons. This value includes a correction of 9% due to perturbations of an excited state about 1900 cm^{-1} above the ground-state doublet of Pa^{4+} in its octahedral crystal field. A lower frequency double-resonance experiment is used to measure the weak hyperfine interaction of the Pa^{4+} ion with its Cs^{133} neighbors, of order $A''/h \approx 0.5$ Mc/sec.

INTERACTION OF SLOW ELECTRONS WITH INSULATING CRYSTALS. II. COMPARISON OF ELECTRON AND PHOTON ABSORPTION COEFFICIENTS FOR KCl AND KBr. William J. Fredericks and Charles J. Cook, Stanford Research Institute, Menlo Park, California (Received October 28, 1960).

The electron absorption coefficient for pure KCl and additively colored KCl and KBr was measured in the energy range from 0.2 to 12 ev. These data are compared with photon absorption measured in the same crystals in the energy range from 1.2 to 6.5 ev and with published optical and photoemission data above 6.5 ev. Certain imperfection interactions were found at corresponding photon and electron energies. The surface transition layer, even for pure KCl, was observed to contain F and V_3 centers. There was no evidence of direct electron-exciton interactions. The valence band of KCl was observed to be 8.6 ± 0.2 ev below the vacuum level; this agrees with Eby, Teegarden, and Dutton's measurements. Upon electron bombardment, an optical absorption near the first fundamental band was found to develop. Its characteristics do not coincide with any of the absorption bands previously reported in this energy region.

VISIBLE LUMINESCENCE OF RARE EARTH-YTTRIUM GALLIUM GARNETS. S. P. Keller and G. D. Pettit, International Business Machines Research Center, Yorktown Heights, New York (Received October 3, 1960).

Yttrium gallium garnet ($Y_3Ga_5O_{12}$) has been prepared with small percentages of different rare earths substituted for yttrium. Garnets

activated with Pr, Sm, Eu, Tb, Dy, Ho, Er, and Tm are all luminescent. The emission and excitation spectra of the samples have been measured at 77°K. The data have been analyzed in terms of the atomic energy levels of the impurity ions and the effects of crystalline field and of phonon interactions. Wherever possible, comments are made about whether the crystal field can be treated as possessing cubic or lower symmetry.

ELECTRICAL RESISTIVITY OF LANTHANUM, PRASEODYMIUM, NEODYMIUM, AND SAMARIUM. J. K. Alstad, R. V. Colvin,* S. Legvold, and F. H. Spedding, Institute for Atomic Research and Department of Physics, Iowa State University, Ames, Iowa (Received November 9, 1960).

The electrical resistivities of polycrystalline samples of La, Pr, Nd, and Sm are reported in the temperature range 1.3°K to 300°K. La exhibits a superconducting transition at 5.8°K. The curve for Pr has slope changes at 61°K and 95°K. The Nd curve shows small jumps at 5°K and 20°K. Sm shows slope changes at 14°K and 106°K.

*Now at the Edgar C. Bain Laboratory of the U. S. Steel Corporation, Monroeville, Pennsylvania.

LOW-TEMPERATURE MAGNETIC SUSCEPTIBILITIES OF THE HYDRATED ACETATES OF Ni^{++}, Co^{++}, AND Mn^{++}. R. B. Flippen* and S. A. Friedberg, Carnegie Institute of Technology, Pittsburgh, Pennsylvania (Received August 9, 1960).

The magnetic susceptibilities of powdered $Ni(C_2H_3O_2)_2 \cdot 4H_2O$, $Co(C_2H_3O_2)_2 \cdot 4H_2O$, and $Mn(C_2H_3O_2)_2 \cdot 4H_2O$ have been measured in the liquid hydrogen and helium ranges by an ac mutual inductance method. Measurements on the cobalt salt were extended to 0.4°K, revealing a sharp maximum at 0.6°K. A similar, more pronounced susceptibility peak is observed in the manganous acetate at 3.2°K. Single-crystal measurements have been made on the latter salt along the monoclinic *b* axis as well as in the *ac* plane in external fields up to 1000 gauss. Saturation and hysteresis are seen in the *a* direction associated with the appearance of a weak ferromagnetic moment below 3.18°K. $Mn(C_2H_3O_2)_2 \cdot 4H_2O$ appears to be a weak ferromagnet of the kind discussed recently by Dzyaloshinsky and Moriya.

*Now at Central Research Department, Experimental Station, E. I. duPont de Nemours and Co., Wilmington, Delaware.

BEHAVIOR OF EXCITED ELECTRONS AND HOLES IN ZINC SULFIDE PHOSPHORS. Shigeo Shionoya,* Hartmut P. Kallmann, and Bernard Kramer,† Department of Physics, New York University, Washington Square, New York, New York (Received October 11, 1960).

The luminescent properties of silver- and copper-activated ZnS phosphors have been investigated at room and liquid air temperatures using ultraviolet, blue light, and β-ray excitation. In many cases it was found that the deficiency area was considerably smaller than the glow-curve area, especially for β-ray excitation of ZnS:Cu. This is explained by the hole production causing quenching during β-ray excitation, while during the glow curve the smaller amount of holes produced causes a much smaller amount of quenching. However, even with blue light where excitation does not directly produce holes, the deficiency area is smaller than the glow-curve area.

The effect of infrared radiation on the fluorescence, phosphorescence, and glow curve has been investigated, and the quenching and stimulation at room and liquid air temperature reported. For ZnS:Cu the long-wavelength infrared band (~12 000 A) produces quenching at room temperature but only stimulation at low temperature.

A determination of trap density from the glow curves shows $\sim 10^{17}/cm^3$ for ZnS:Cu and $\sim 10^{16}/cm^3$ for ZnS:Ag at liquid air temperatures.

Finally, a theoretical discussion of the possible transition mechanisms giving rise to these effects is given.

*Work performed while on leave from Yokohama National University, Yokohama, Japan. Presently associated with The Institute for Solid State Physics, University of Tokyo, Tokyo, Japan.

†Also Department of Physics, Hunter College, New York, New York.

GREEN'S FUNCTION METHOD FOR QUANTUM CORRECTIONS TO THE THOMAS-FERMI MODEL OF THE ATOM. Gene A. Baraff and Sidney Borowitz, Physics Department, New York Uni-

versity, New York, New York (Received August 12, 1960; revised manuscript received December 13, 1960).

A systematic method is presented for deriving the Thomas-Fermi equation for an atom and the quantum corrections from the many-body description. The novel feature of the method is that it does not require any a priori assumptions about the assignment of electrons to fully occupied single-particle states or about the distribution of electrons in phase space, but shows instead that the distribution which is usually assumed, or derived from the assumption of fully occupied single-particle states, is a direct consequence of specifying that the many-particle system is in its ground state. The procedure used in the derivation is the expansion of the mixed position-momentum representation of the Green's function in a series of powers of $\hbar$. The lowest order term is found to correspond with the Thomas-Fermi density. The form of the higher order terms, which are to be considered as corrections to zeroth order term, depends on the approximations made in the many-body equations for obtaining the Green's function. This paper deals only with the Hartree-Fock approximation, but the methods presented here allow generalization to other approximations which can include correlation effects.

ENERGY DISTRIBUTION OF ELECTRONS FROM IONIZING COLLISIONS OF HEAVY PARTICLES. H. W. Berry, Syracuse University, Syracuse, New York (Received October 17, 1960).

The energy distribution of electrons produced in ionizing collisions of ions and fast atoms with atoms of the parent gas at rest has been measured for A and He. The energy of the incident particles ranged from 0.30 to 3.0 kev. Electrons released at 90° with the incident ion or atom beam were analyzed in an electrostatic energy selector which consisted of 90° segments of coaxial cylinders. The use of a fine wire grid in the region in which the ionization occurred allowed a positive differentiation to be made between the ionization electrons and the secondary electrons from any metal surfaces. The electron distributions for argon ions and atoms in argon are similar and show a rapid decrease in the yield as the energy increases from zero to about 4 ev followed by a plateau and a flat maximum near 12 ev. The distributions for He also show the initial rapid decrease continuing to a small maximum which for the ion is at about 31 ev and for the neutral atom at about 16 ev. These distributions are almost collision energy independent, though with an increase in the over-all yield with increasing energy.

ISOTOPE SHIFTS IN PALLADIUM. R. H. Hughes and F. A. Sharpton,* Physics Department, University of Arkansas, Fayetteville, Arkansas (Received November 14, 1960).

Isotope shifts in the $4d^9\,5s\ {}^1D_2 - 4d^9\,5p\ {}^3F_3{}^\circ$ transition at $\lambda 4212$ A in the first spectrum of Pd have been studied with the use of enriched isotopes. The shifts are similar to those found by Kuhn and Warner in the $4d^9\,5s\ {}^3D_3 - 4d^9\,5p\ {}^3F_4{}^\circ$ transition at $\lambda 3405$ A. The most interesting feature is the maximum in the isotope shift which appears at the neutron number pair 60-58.

*Now at Hendrix College, Conway, Arkansas.

BOUNDS ON SCATTERING PHASE SHIFTS FOR COMPOUND SYSTEMS. Leonard Rosenberg and Larry Spruch, Physics Department, Washington Square College and Institute of Mathematical Sciences, New York University, New York, New York (Received November 9, 1960).

An extension of recently developed methods determines a rigorous upper bound on $(-k\ \cot\eta)^{-1}$, where η is the phase shift, for the general one-channel scattering process. The method unfortunately requires truncation of the various potentials, but it should generally be possible, in practice, to so truncate the potentials that the difference between the phase shifts of the original problem and of the problem for which a bound is obtained is insignificant.

In the course of the development it is necessary to introduce, for compound-system scattering, an absolute definition of the phase shift, not simply a definition modulo π. The definition chosen is to take the projection of the full scattering wave function on the ground-state wave function of the scattering system, and to treat the resultant one-coordinate wave function as if it were the scattering wave function for a particle on a center of force. Though irrelevant with regard to the determination of a bound on $\cot\eta$, it is interesting that at least for some simple cases this definition automatically in-

creases the phase shift by at least π whenever the Pauli principle introduces a spatial node into the scattering wave function. The triplet scattering of electrons by hydrogen atoms provides an example.

ISOTOPE SHIFT IN THE ARC SPECTRUM OF NICKEL. Daniel J. Schroeder and J. E. Mack,* University of Wisconsin, Madison, Wisconsin (Received September 19, 1960).

The isotope shift in 31 spectral lines in the nickel arc spectrum has been determined by the use of a Fabry-Perot interferometer. The normal mass shifts were calculated ($\approx +0.025$ cm^{-1} between Ni^{58} and Ni^{64}) and subtracted from the observed isotope shifts. The differences were attributed to the specific mass and field effects. The relative shifts of levels of four configurations were deduced from the observed line shifts, these being the "complex" configurations, $3d^8 4s^2$ and $3d^8 4s 4p$, and the two-electron configurations, $3d^9 4s$ and $3d^9 4s$. It was shown that the shifts due to the specific mass effect are a significant part of the observed shifts. Perturbations due to interconfiguration interactions were postulated to explain some of the observed shifts. The isotope shift to be expected between Ni^{58} and Ni^{64} on the basis of field-effect calculations is about -0.020 cm^{-1} for a single 4s electron, while the shifts observed are as large as $+0.190$ cm^{-1}. A large fraction of this shift must therefore be attributed to the specific mass effect. By noting the deviations of the relative shifts between adjacent pairs of even isotopes from those predicted by mass-effect theory, it was possible to deduce the relative field effect. The relative level shift resulting from the field effect is nearly the same for the adjacent isotope pairs, 60-62 and 62-64, while the relative level shift for the isotope pair, 58-60, is approximately 0.004 cm^{-1} larger than that for the other adjacent isotope pairs. The arrangement of neutrons in the outermost nuclear shells is believed to account for this difference. Within the experimental error the level shift of the Ni^{61} relative to the neighboring even isotopes is such that there is no odd-even staggering of the levels.

*Currently on leave as Scientific Attaché, Stockholm, Sweden.

ANALYSIS OF GAMMA-GAMMA POLARIZATION-DIRECTIONAL CORRELATIONS INVOLVING MULTIPOLE MIXTURES. M. B. Martin, R. G. Arns, and M. L. Wiedenbeck, Harrison M. Randall Laboratory of Physics, The University of Michigan, Ann Arbor, Michigan (Received August 19, 1960).

A method is described for the graphical analysis of the gamma-gamma polarization-directional correlation when one or both gamma rays involve a mixture of dipole and quadrupole radiation. The case in which the polarization of the mixed gamma ray is observed is treated in detail.

STATISTICAL THEORY OF GAMMA-RAY SPECTRA FOLLOWING NUCLEAR REACTIONS. E. S. Troubetzkoy, Nuclear Development Corporation of America, White Plains, New York (Received October 18, 1960).

A theory predicting γ-ray spectra following intermediate or high-energy nuclear reactions is derived on the basis of the statistical theory. The equations take a particularly simple form if the assumption is made that all radiative transitions are of the electric dipole type. The theory is applied to two specific reactions: inelastic neutron scattering and thermal neutron capture. Numerical calculations of spectra arising from thermal neutron capture by two gadolinium isotopes are shown to compare well with experiments.

NEUTRON-CAPTURE GAMMA-RAY SPECTRA OF THE NICKEL ISOTOPES. P. A. Treado and P. R. Chagnon, Physics Department, The University of Michigan, Ann Arbor, Michigan (Received September 14, 1960).

The spectra of gamma radiation following pile-neutron capture in separated isotopes of nickel have been measured with a three-crystal scintillation pair spectrometer as well as with a single-crystal scintillation counter. Energies and intensities of the gamma rays from each isotope are reported. Each of the lines observed with natural nickel has been assigned to $Ni^{58}(n,\gamma)Ni^{59}$, $Ni^{60}(n,\gamma)Ni^{61}$, or $Ni^{62}(n,\gamma)Ni^{63}$. In some cases, gamma rays of nearly identical energies are found in two, or in all three, isotopes. Additional

gamma rays not resolved in the natural nickel spectrum appear in $Ni^{58}(n,\gamma)Ni^{59}$ at 7.65 Mev, and in $Ni^{60}(n,\gamma)Ni^{61}$ at 4.70 and 5.55 Mev. The spectrum of $Ni^{62}(n,\gamma)Ni^{63}$ is dominated by a strong line at 6.80 Mev, presumably the ground-state transition.

ELASTIC SCATTERING OF ALPHA PARTICLES BY N^{15}. H. Smotrich, K. W. Jones,* L. C. McDermott, and R. E. Benenson,† Columbia University, New York, New York (Received August 24, 1960).

Absolute differential cross sections for the elastic scattering of alpha particles by N^{15} have been measured in a differentially-pumped gas scattering chamber. The measurements were made at center-of-mass angles of 169.1, 149.5, 140.8, 125.3, 90.0, and 70.0 degrees for alpha-particle energies from 1.75 to 5.50 Mev, corresponding to 5.37- to 8.33-Mev excitation of the compound nucleus F^{19}. The experimental widths of the levels observed below approximately 3.5-Mev bombarding energy are generally narrow, in most cases less than 10 kev. Above 3.5 Mev a marked increase in the level width was observed. As a result of an analysis based on the Wigner-Eisenbud reaction theory, values of J, π, E_λ, and $\gamma_\lambda{}^2$ were assigned to 16 levels in F^{19}.

*Now at the Ohio State University, Columbus, Ohio.
†Permanent address: City College of New York, New York, New York.

ANALYSIS OF LONG-RANGE ALPHA-EMISSION DATA. R. D. Griffioen and J. O. Rasmussen, Lawrence Radiation Laboratory, University of California, Berkeley, California (Received November 2, 1960).

Alpha barrier penetrabilities for the long-range alphas of Po^{212} and Po^{214} are calculated by using the diffuse exponential nuclear potential derived from optical-model analysis of alpha elastic-scattering data. The calculations are made on the same basis as reported by Rasmussen in two previous publications. Partial half-lives for alpha and gamma emission are calculated on the assumption that the long-range alpha decay is unhindered with respect to the ground-state alpha decay.

METHOD TO OBTAIN THE ENERGY DEPENDENCE OF REACTION CROSS SECTIONS WHEN A COMPOUND NUCLEUS IS FORMED. Raymond Fox and Richard D. Albert, Lawrence Radiation Laboratory, University of California, Livermore, California (Received November 10, 1960).

It is found that measuring the energy distributions of emitted particles at two different incident energies and two reaction cross sections is sufficient to obtain the energy dependence of a reaction cross section when it is known that a compound nucleus is formed. The cross sections obtained are a function of the excitation energy of the residual nucleus. They are the usual reaction cross sections at zero excitation energy when the assumption is made that the reaction cross section does not vary with the excitation energy of the target nucleus. By comparing the reaction cross sections thus obtained with measured nonelastic cross sections, the compound elastic cross section may also be obtained. An example using this method is given in which two measured energy distributions and two measured cross sections were used to obtain the energy dependence of the reaction cross section of nickel in the 2.5- to 7-Mev energy range.

ENERGY LEVELS IN Zr^{91} EXCITED BY THE (d,p) REACTION. R. L. Preston,* H. J. Martin, Jr.,† and M. B. Sampson, Indiana University, Bloomington, Indiana (Received November 3, 1960).

Eleven energy levels in Zr^{91} were excited. The excitation energies of the levels are 0, 1.22, 2.07, 2.19, 2.56, 2.84, 3.05, 3.25, 3.45, 3.65, and 3.87 Mev. Angular distributions were measured for the first four levels and assignments were made using the shell model and the Butler stripping theory. The assignments are $2d_{5/2}$ for the ground state, $3s_{1/2}$ for the 1.22-Mev state, $2d_{3/2}$ for the 2.07-Mev state, and $1g_{7/2}$ for the 2.19-Mev state. The application of the Butler theory to the data gave reasonable and useful fits. The ground-state Q value was measured and is 5.02 ± 0.03 Mev.

*Present address: 35 Bedford Park Avenue, Richmond Hill, Ontario, Canada.
†Now on leave at the Brookhaven National Laboratory, Upton, New York.

NATURAL ALPHA RADIOACTIVITY IN MEDIUM-HEAVY ELEMENTS. Ronald D. Macfarlane* and Truman P. Kohman, Department of Chemistry, Carnegie Institute of Technology, Pittsburgh, Pennsylvania (Received November 14, 1960).

A large cylindrical ionization counter accomodating samples up to 1200 cm^2 in area has been used for measurements of natural alpha radioactivity in medium-heavy elements. Low-background techniques and multichannel pulse analysis are employed. The method has greater energy resolution and yields better counting statistics than the nuclear emulsion technique, but does not have as great a sensitivity. The results obtained from measurements on natural elements and isotopically enriched samples are:

Nuclide	Alpha particle energy (Mev)	Specific activity of natural element (dis sec^{-1} g^{-1})	Half-life or limit for nuclide (years)
Ce^{142}	...	<0.0002	$>5\times10^{16}$
Nd^{144}	1.83 ±0.02	0.0093 ±0.0011	$(2.4\pm0.3)\times10^{15}$
Sm^{146}	...	<0.013	$<3\times10^{8}$
Sm^{147}	2.23 ±0.02	116 ±5	$(1.15\pm0.05)\times10^{11}$
Sm^{148}	...	<0.04	$>2\times10^{14}$
Sm^{149}	...	<0.01	$>1\times10^{15}$
Gd^{152}	2.14 ±0.03	0.00156 ±0.0010	$(1.08\pm0.08)\times10^{14}$
Hf^{174}	2.50 ±0.03	0.000065 ±0.000013	$(2.0\pm0.4)\times10^{15}$
W^{180}	...	<0.00013	$>9\times10^{14}$
Pt^{190}	3.11 ±0.03	0.012 ±0.001	$(6.9\pm0.5)\times10^{11}$
Hg^{196}	...	<0.0007	$>1\times10^{14}$

*Present address: Lawrence Radiation Laboratory, University of California, Berkeley, California.

PREDICTIONS OF SPONTANEOUS FISSION HALF-LIVES FOR HEAVY NUCLEI. David W. Dorn, Lawrence Radiation Laboratory, University of California, Livermore, California (Received November 4, 1960).

Swiatecki's work on correlation of spontaneous fission half-lives has been modified and extended to include elements beyond $Z=100$. The values of spontaneous fission half-lives predicted on these bases are unexpectedly high. For example, the partial half-life for $Z=106$, $A=271$ is predicted to be about 13 years.

DECAY OF 49-min Cd^{118} AND 5.1-sec In^{118}. Chester E. Gleit* and Charles D. Coryell, Department of Chemistry and Laboratory for Nuclear Science, Massachusetts Institute of Technology, Cambridge, Massachusetts (Received November 2, 1960).

The decay properties of 49-min Cd^{118} and its daughter 5.1-sec In^{118} are established. The Cd^{118} has a low β-decay energy and seems to be an allowed transition. The In^{118} has (4.2 ± 0.4)-Mev β-decay energy, with about 15% of the decays going to the 1.22-Mev excited state of Sn^{118}, both β transitions being allowed. It is proposed that a previously identified 4.5-min In species is a high-spin isomer In^{118m} not formed in the β decay of Cd^{118} or formed directly in uranium fission.

*Present address: Westinghouse Electric Corporation, Bettis Atomic Power Laboratory, Pittsburgh, Pennsylvania.

DECAY OF Ne^{18}. J. W. Butler and K. L. Dunning, Nucleonics Division, U. S. Naval Research Laboratory, Washington, D. C. (Received November 2, 1960).

The radioactive nuclide Ne^{18} has been produced in the $O^{16}(He^3,n)Ne^{18}$ reaction by 5.2-Mev He^3 particles from the NRL 5-Mv Van de Graaff accelerator. The target, CaO on a Pt backing, was about 300 kev thick to the incident beam. The gamma rays following the decay of Ne^{18} were detected by a 3-in. diam by 3-in. NaI(Tl) crystal and a 256-channel pulse-height analyzer.

Only one nuclear gamma ray was observed. Its energy, measured with respect to the Na^{22} gamma ray at 1.2736 ± 0.0016 Mev, is 1.041 ± 0.005 Mev. Therefore, this gamma ray is assigned to the 1.04-Mev state of F^{18}. This state is considered to be the isobaric spin analog state of the Ne^{18} ground state, and therefore has quantum parameters 0^+, $T=1$. The branching to this excited state was measured to be 0.07 ± 0.02 (including a calculated contribution of 0.00006 from orbital electron capture), and that to the ground state of F^{18} was measured to be 0.93 ± 0.02 (including a calculated contribution of 0.0002 from orbital electron capture). The *ft* values are, respectively, 3030 ± 880 and 1120 ± 70 sec. The half-life of Ne^{18} was measured to be 1.46 ± 0.07 sec.

O^{14} DECAY ENERGY AND THE FERMI INTERACTION CONSTANT. J. W. Butler and R. O. Bondelid, Nucleonics Division, U. S. Naval Research Laboratory, Washington, D. C. (Received November 10, 1960).

The threshold energy of the $C^{12}(He^3,n)O^{14}$ reaction has been measured precisely with the use of a Van de Graaff accelerator and an electrostatic analyzer, the value being 1436.2 ± 0.9 kev. From this value, the O^{14} beta-decay end-point energy (for decay leading to the 2.312-Mev state in N^{14}) is computed to be 1.8000 ± 0.0065 Mev, based on the 1956 table of masses, and 1.8097 ± 0.0015 Mev, based on the 1960 table of masses. A revised value of the Fermi interaction constant in beta decay is calculated and applied in the conserved-vector-current theory of Feynman and Gell-Mann. When (1) the radiative corrections and other corrections are applied to the decay of O^{14}, (2) the corrected *ft* value is used to compute the vector coupling constant in beta decay, (3) the value of this vector coupling constant is assumed to be the same as that for the muon decay and is used to calculate the lifetime of the muon, and (4) this lifetime is corrected for radiation effects, the predicted mean life of the muon becomes 2.289 ± 0.013 μsec (based on the 1960 table of masses and the radiative corrections of Kinoshita and Sirlin) or 2.245 ± 0.013 μsec (based on the 1960 table of masses and the corrections, radiative and otherwise, of Durand and collaborators). The former value is 3.6% greater than a weighted average of several recent measurements of the muon mean life, 2.210 ± 0.003 μsec, while the latter value is only 1.6% greater, and is within the combined experimental and theoretical uncertainties. However, the definitions of coupling constants used by Durand and collaborators differ somewhat from those used by others.

PHOTOPRODUCTION AND DETECTION OF THE TWO-MESON BOUND STATE. Jack L. Uretsky and T. R. Palfrey, Jr., Purdue University, Lafayette, Indiana (Received August 3, 1960; revised manuscript received December 14, 1960).

We investigate the possibility of the detection of a photoproduced two-pion bound system. The general detection problem is discussed briefly; the branching ratio between $2\pi^0$ and $2\gamma^0$ decay modes is calculated; and the total photoproduction cross section is estimated in terms of the binding energy of the two-pion state both by field-theoretic and by phase-space arguments. We conclude that if the binding energy is of the order of 10 Mev the state should be detectable in photoproduction experiments, and the binding energy should be measurable.

EXCITATION FUNCTIONS OF $(p, 2$ NUCLEON) REACTIONS. P. P. Strohal* and A. A. Caretto, Jr., Department of Chemistry, Carnegie Institute of Technology, Pittsburgh, Pennsylvania (Received September 26, 1960; revised manuscript received December 5, 1960).

Excitation functions for the (p,pn) reaction have been determined in the energy range 250 Mev to 440 Mev for the target nuclei As^{75}, Br^{81}, Zr^{96}, I^{127}, Ce^{142}, W^{186}, and Re^{187}. Both isomer products were determined in the case of the $Br^{81}(p,pn)Br^{80}$ reaction. Also, excitation functions were determined for the $(p,2p)$ reaction on Zr^{96}, Ce^{142}, and W^{186} and for the $(p,2n)$ reaction on Zr^{96}. All cross sections were measured relative to the $Al^{27}(p,3pn)Na^{24}$ excitation function. The (p,pn) excitation functions are only moderately sensitive to energy, showing an increase by about 30% for iodine, 20% for arsenic and cerium, and a 12% decrease for zirconium. The remaining excitation functions are flat. The ratio of the $\sigma_{p,pn}$ to $\sigma_{p,2p}$ is 1.62 ± 0.09, for the three targets measured at 440 Mev. The various mechanisms for the production of reactions of this type are examined in the light of present

understanding. The suggestion is made that, despite the relative insensitiveness of these excitation functions to energy, (p,pn) and $(p,2p)$ reactions may take place by more than one mechanism in this energy region. A comparison is made with the results of recent Monte Carlo nuclear cascade calculations applied to calculation of (p,pn) reaction excitation functions.

*Present address: Institut Ruder Boskovic, Zagreb, Yugoslavia.

RADIATIVE DECAY MODES OF THE MUON. R. R. Crittenden and W. D. Walker, University of Wisconsin, Madison, Wisconsin, and J. Ballam, Michigan State University, East Lansing, Michigan (Received August 29, 1960).

A 5-in. Freon bubble chamber was used to search for the following decay modes of the μ^+ meson:

$$(1)\ \mu^+ \to e^+ + \gamma,$$

$$(2)\ \mu^+ \to e^+ + e^- + e^+,$$

$$(3)\ \mu^+ \to e^+ + \nu^0 + \bar{\nu}^0 + \gamma,$$

$$(4)\ \mu^+ \to e^+ + \nu^0 + \bar{\nu}^0 + e^+ + e^-.$$

Two exposures were made at the Carnegie Institute of Technology synchrocyclotron. A total of 200 000 pictures were taken, yielding 3.3×10^5 μ^+-meson decays.

A total of 3×10^5 μ^+ decays were examined for mode (1). No decays consistent with this mode were found. The upper limit on the branching ratio R_{rad} was found to be

$$R_{\text{rad}} = (\mu^+ \to e^+ + \gamma)/(\mu^+ \to e^+ + \nu^0 + \bar{\nu}^0) < 2.5\times10^{-5}.$$

A total of 3.3×10^5 μ^+ decays were scanned for mode (2) and no such decays were observed. The limit on the branching ratio R_{3e} was found to be

$$R_{3e} = (\mu^+ \to e^+ + e^- + e^+)/(\mu^+ \to e^+ + \nu^0 + \bar{\nu}^0) < 4\times10^{-6}.$$

The internal bremsstrahlung rate (mode 3) was measured for two values of $E_{\gamma 0}$ (the minimum photon energy detected). The results were

$$R_{\text{IB}} = (\mu^+ \to e^+ + \nu^0 + \bar{\nu}^0 + \gamma)/(\mu^+ \to e^+ + \nu^0 + \bar{\nu}^0);$$

$$R_{\text{IB}} = (1.4\pm0.4)\times10^{-2}, \quad E_{\gamma 0} = 10 \text{ Mev};$$

$$R_{\text{IB}} = (3.3\pm1.3)\times10^{-3}, \quad E_{\gamma 0} = 20 \text{ Mev}.$$

The rate of internal conversion of internal bremsstrahlung (mode 4) was found to be

$$R_{\text{IC}} = (\mu^+ \to e^+ + \nu^0 + \bar{\nu}^0 + e^+ + e^-)/(\mu^+ \to e^+ + \nu^0 + \bar{\nu}^0)$$

$$= (2.2\pm1.5)\times10^{-5}, \quad E_0 = 10 \text{ Mev},$$

where E_0 is the minimum energy of the internally converted γ ray.

A summary is given of previous experiments on these decay modes and results are discussed with special reference to the intermediate-boson scheme of weak four-fermion interactions.

CLOUD-CHAMBER STUDY OF HARD COLLISIONS OF COSMIC-RAY MUONS WITH ELECTRONS. R. F. Deery* and S. H. Neddermeyer, Department of Physics, University of Washington, Seattle, Washington (Received November 1, 1960).

The energy distribution of the secondary electrons produced in targets of carbon or paraffin by the μ-e scattering process for muon momenta in the range 5-50 Bev has been measured for electron energies up to 20 Bev, or c.m. momentum transfer up to 140 Mev. A vertical array of three cloud chambers immersed in a magnetic field of 11 000 gauss was used with a fourfold coincidence system. Two flat rectangular proportional counters, suitably biased, together with two Geiger-Müller trays, provided fair rejection of uneventful penetrating particles and a high efficiency for selection of the narrow electronic showers characteristic of the high-energy electromagnetic events. On 5900 counter-triggered photographs there were 291 accepted events, having one or more (±) electrons with energy ≥ 0.10 Bev, believed to originate in μ-e collisions in the (carbon or paraffin) target above the top chamber, from incident muons in the momentum interval 5-50 Bev. The data are compared with a calculation based on the Bhabha formula for spin 1/2 muons, taking into account the momentum distribution of the incident muons, the energy loss and shower development in the target and the chamber walls, and a theoretical efficiency factor. Arguments are given to show that direct pair production and bremsstrahlung of the muons in the target and in the Pb shield above the apparatus produce negligible effects. The experiment permits a reliable measurement of only the relative distribution. When arbitrarily normalized, the calculated distribution is in

fairly good agreement with the data, except for a small systematic difference suggesting an excess of observed events for the harder collisions. Although the discrepancy is interpretable as a statistical fluctuation, the data are fitted much better over the entire range when the basic cross section is modified by a "form factor," F^2 (greater than unity), with $F = 1 + |q^2|\lambda_\mu^2$, where q is the invariant of the 4-momentum transfer in units of $\hbar$, and λ_μ is the Compton wavelength of the muon. This may be the first indication of a deviation from standard quantum electrodynamics for hard μ-e collisions. More strongly it shows that, if there is a deviation, it is not representable by a form factor less than unity.

*Now at the California Institute of Technology, Pasadena, California.

SPIN IN CLASSICAL AND QUANTUM THEORY. H. C. Corben, Space Technology Laboratories, Los Angeles, California (Received March 31, 1960; revised manuscript received October 13, 1960).

The classical equations of motion of a charged point particle with intrinsic spin under the influence of an external electromagnetic field are restated and compared with the Heisenberg equations of motion derived from the Dirac theory. The partition of angular momentum between particle and field in the classical theory is contrasted to the Dirac theory of electron spin. The analogy between the Dirac equation and the theory of parametric amplification is pointed out.

A free spinning point particle moving according to the laws of classical relativistic point-particle mechanics may move along a helix. The sum of the intrinsic spin σ and the angular momentum of the helical motion in this classical analog of Zitterbewegung is an effective spin vector S which is a constant of the motion. Because of this internal motion, the effective mass M of the particle differs from the mass m which is ascribed to it in the equations of motions. Solutions are found in which S is parallel or antiparallel to the momentum, and the sign of M is determined by the helicity. When placed in a uniform electromagnetic field, the particle behaves as if it had a rest mass M and a magnetic moment $e\sigma/Mc$, in addition to any explicit magnetic moment that may be ascribed to it.

CONTINUATION OF SCATTERING AMPLITUDES AND FORM FACTORS THROUGH TWO-PARTICLE BRANCH LINES. Reinhard Oehme, Enrico Fermi Institute for Nuclear Studies and Department of Physics, University of Chicago, Chicago, Illinois (Received November 3, 1960).

It is shown that scattering amplitudes and form factors have two-particle branch lines which connect two Riemann sheets. For partial wave amplitudes and form factors the dispersive parts and, except for square root factors, the absorptive parts are regular functions in the cut energy plane except for isolated poles, physical inelastic cuts, and left-hand branch lines. In order to show this it is assumed that, for particles without composite structure, the amplitudes have only such singularities in the physical sheet which correspond to absorptive processes. The analytic properties of absorptive parts are used for a general discussion of structure singularities (anomalous thresholds). It is shown that these structure cuts are extensions of left-hand branch lines. An example is given of a dispersion relation on the Riemann surface in which the integral over the two-particle branch line is eliminated.

RELATIVISTIC PARTICLE DYNAMICS. B. Bakamjian, The Pennsylvania State University, University Park, Pennsylvania (Received November 10, 1960).

It is shown that an instant form of relativistic particle dynamics can be constructed which displays the symmetry properties inherently present in the point form. In this new instant form, interaction terms are introduced in the energy-momentum four-vector of the system; physically this is more justifiable than the more customary method of having interaction terms appear in the energy and the three generators of the Lorentz group which give the three infinitesimal displacements in velocity.

DYNAMICAL MODEL OF ELEMENTARY PARTICLES BASED ON AN ANALOGY WITH SUPERCONDUCTIVITY. I. Y. Nambu and G. Jona-Lasinio,* The Enrico Fermi Institute

for Nuclear Studies and the Department of Physics, The University of Chicago, Chicago, Illinois (Received October 27, 1960).

It is suggested that the nucleon mass arises largely as a self-energy of some primary fermion field through the same mechanism as the appearance of an energy gap in the theory of superconductivity. The idea can be put into a mathematical formulation utilizing a generalized Hartree-Fock approximation which regards real nucleons as quasi-particle excitations. We consider a simplified model of nonlinear four-fermion interactions which allows a γ_5-gauge group. An interesting consequence of the symmetry is that there arise automatically pseudoscalar zero-mass bound states of a nucleon-antinucleon pair which may be regarded as an idealized pion. In addition, massive bound states of nucleon number zero and two are predicted in a simple approximation.

The theory contains two parameters which can be explicitly related to the observed nucleon mass and the pion-nucleon coupling constant. Some paradoxical aspects of the theory in connection with the γ_5 transformation are discussed in detail.

*Fulbright Fellow, on leave of absence from Istituto di Fisica dell'Università, Roma, and Istituto Nazionale di Fisica Nucleare, Sezione di Roma, Italy.